PHOTOCATALYTIC DEGRADATION OF TRYPAN BLUE USING GOLD/TITANIUM DIOXIDE

INTRODUCTION

Wastewater produced from textile and other dyestuff industrial process contains large quantities of organic compounds that present an increasing environmental contaminations. Indeed, about 1-20% of total world production of dyes is lost during the dying process and released into effluents (Konstantinou and Albanis, 2004). Azo dyes which contain one or more nitrogen to nitrogen double bonds are widely used in the dyeing industries, approximately 50-70% of the dyes available on the market are azo compounds (Bauer *et al.*, 2001). Moreover, some azo dyes and their degradation products have been found or suspected to be human carcinogens (Stylidi *et al.*, 2003). Therefore, decolorisation and detoxicity of dyes effluents have received increasing attention.

Regarding traditional techniques for wastewater treatment physical, biological and chemical methods are known (Slokar and Marechal, 1998). Each method has few advantages and disadvantages. For example, physical methods are technically easy and low cost process but nondestructive, that is they just transfer the pollutants from aqueous solution to another phase rather than destroy them. Consequently, these methods are only color removal including coagulation, filtration and activated carbon adsorption etc. Biological methods by living organisms or fungi are ineffective to degrade dyes if the large, chemical refractory and stable molecule of aromatics compounds present in dyes, so treatment can not base on biodegradation alone. Advanced Oxidation Processes (AOPs) are based on the generation of very reactive species such hydroxyl radical ($^{\bullet}OH$) that oxidize a broad range of pollutants quickly and non selectively (Konstantinou and Albanis, 2004). Among AOPs, heterogeneous photocatalysis is an attractive method which is a combination of photochemistry and catalysis to bring out a chemical reaction. The optimal photodegradation has to be successfully employed to completely degrade of various organic pollutants and may lead to total mineralization of organic compounds to carbon dioxide, water, mineral acid and inorganic ions (Sakthivel *et al.,* 2003).

In the past few years, many catalysts like TiO_2, ZnO, WO_3, SnO_2, ZrO_2, CeO_2, CdS and ZnS have been used for photodegradation. When these semiconductor particles are illuminated with photons using the light source, the absorption of light is followed by formation of electron-hole pairs at the surface of the semiconductor. Electrons on the surface are excited to the conduction band whereas positive holes are formed in the valence band. Afterwards the holes react with electron donors in the solution to produce powerful oxidizing free radicals such as hydroxyl radical, which oxidize the organics on the surface. The excited electrons and holes can react with the adsorbed species on the semiconductor's surface. The photogenerated electron-hole pairs can oxidize a number of species present in the solution efficiently (Tang and An, 1995). Although, TiO_2 has been proved to be an excellent catalyst, low cost and chemical stability (Reutergardn and Iangphaluk, 1997 and Hu *et al.,* 2003), there are still a few drawbacks of using TiO_2: i) the band gap of 3.2 eV, it can be activated only UV light, ii) charge carrier recombination occurs within nanoseconds and iii) in case of aqueous powder dispersions, the cost of separating TiO_2 after treatment is high (Sakthivel *et al.*, 2004). To utilize sunlight or visible light and to solve both low rate of degradation and high recombination rate of electron-hole pairs, many researchers have reported that the addition of groups VIII metals and transition metals to TiO_2-based photocatalyst are effective ways to enhance reaction rate (Li, F.B. and X.Z. Li, 2002). To solve the third problem, catalyst powder is loaded on the support such as glass slides, glass bead and alumina etc., but photocatalytic efficiency decreased because of low reaction interfacial area (Sakthivel *et al.,* 2002).

The objects of this research are to develop new composite immobilized photocatalysts, consisting of gold particles deposited on nanocrystalline TiO_2 for treatment of Trypan Blue (Direct Blue 14, Figure 1) employing the solar light simulating source (Xe-arc lamp, 150W). Furthermore, the developed photocatalysts are applied to use under the natural sunlight and treat wastewater samples.

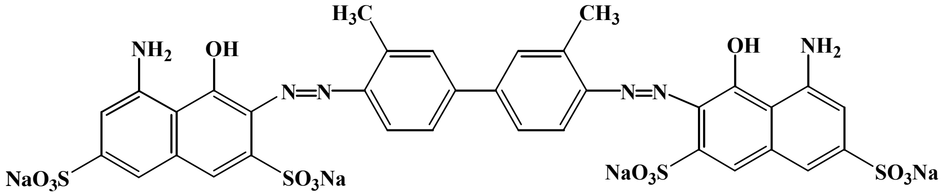

Figure 1 Structural formula of Trypan Blue (Direct Blue 14)

LITERATURE REVIEW

There are a lot of textile wastewater treatment processes including biodegradation methods, various physical methods such as phase-separation, and chemical methods. Nevertheless, none of them is completely satisfactory, for example, phase-separation process with adsorption on activated carbon does not remove or degrade pollutants from the environment. Biological methods are ineffective to degrade pollutants. It is difficult to destroy contaminants containing large, stable and refractory compounds of dyes. Chemical oxidation methods, namely, advanced oxidation processes (AOPs), which generate hydroxyl radicals, are useful in the degradation and transformation of wide range of pollutants. These techniques are the use of H_2O_2 with or without UV irradiation, ozonation, O_3/UV treatment, Fenton's reagent treatment and semiconductor-assisted photocatalytic degradation. Although ozone has high oxidation potential ($E° = +2.078$), it alone reacts very slowly with various compounds. The improved treatment methods involve a combination of ozone with UV light. However, a major problem of this process is the high cost of treatment. AOPs consist of homogeneous oxidation (H_2O_2 and Fenton's reagent treatment) and heterogeneous oxidation using semiconductor. Both homogeneous and heterogeneous catalytic reactions usually are carried out under ultraviolet or visible light, many reported publications emphasized that heterogeneous photocatalytic oxidation overcomes homogeneous photooxidation which adding oxidizing solutions. Main disadvantage of homogeneous processes is their oxidants are consumed, whereas heterogeneous photocatalysis may be reused or fixed on some materials for extended periods and for easy gathering (Halmann, 1996).

Heterogeneous photocatalytic degradation using semiconductor particles as catalysts is an effective technique. Among the available semiconductors, TiO_2 is attractive since it is stable, insoluble, non-toxic, resistant to corrosion and inexpensive. However, it is activated slowly under visible or sunlight, especially sunlight which is an inexpensive source. The limit of combined TiO_2 photocatalysts with visible light is requirement of photosensitizer property of dyes. ZnO is generally unstable and only responsive to UV light. Although WO_3 is useful in visible light, it is less photocatalytically active than TiO_2. CdS can be excited by visible light, but the efficiency of the recycled CdS is significantly lower than TiO_2, as well as photocorrosion.

Consequently, noble metals including group VIII metals and transition metals, e.g. Pt, Pd, Ag (Hu *et al.,* 2003) and Au doped or deposited on TiO_2 have studied to enhance the photocatalytic reaction rate and electron-hole separation, and to extend the light absorption from UV region into the visible or sunlight range as well.

In addition, photocatalytic decolorisation of various specific dyes has been studied under different working conditions. The mineralization or decreases in toxicity of dyes are monitored. The success of mineralization process is complete oxidation of textile dyes to CO_2, H_2O, mineral acid and inorganic ions. Another drawback of TiO_2 is ultrafine TiO_2 powder, so it is too difficult to effectively separate TiO_2 powder from aqueous solution in order to reuse TiO_2. Thus, TiO_2 has been loaded on the various supports. The photocatalytic degradation of various azo dyes, which may be decomposed into potential carcinogenic amines under anaerobic conditions in the environment, has been studied. The effective process used for treatment of an azo dye is focused on heterogeneous photocatalytic degradation using TiO_2 semiconductor. However, none of the treatment approaches ideal process. An ideal waste treatment process will completely mineralize all the toxic species without leaving behind any hazardous residues and it should also be cost effective. The photocatalytic degradation of azo dyes focusing on TiO_2, semiconductor under irradiation of light such as UV, visible and sunlight are reported.

Review of various techniques used in wastewater treatment

Venkatadri and Peters (1993) discussed the application status and potential of three chemical oxidation treatment methods which generate powerful oxidants (hydroxyl radicals): UV/H_2O_2 process, Fenton' s reagent treatment and TiO_2-assisted photocatalytic degradation. These oxidation methods could effectively degrade and mineralize contaminants ranging from inorganic compounds to aliphatic and complex aromatic compounds. Mechanism, kinetics, process improvements, advantages and disadvantages of each method were described. They found that the TiO_2-assisted photocatalytic process could be improved efficiency, applicability and economics for groundwater treatment, especially with the use of solar illumination.

Shu and Huang (1995) studied the chemical oxidation of eight non-biodegradable azo dyes by ozonation and photooxidation processes. In experiments with ozone bubbling, they found that the degradation of azo dyes occurred in the absence of UV light. The degradation rate of azo dyes was observed to be first order with respected to both azo dye and ozone concentrations. The pH of the solution decreased while the azo dyes degraded. No degradation was observed when the azo dye solution was irradiated by UV light alone. The decomposition rates of azo dyes in UV/O_3 photooxidation reactor were much higher than reaction with UV radiation alone and UV/H_2O_2 system. They also discussed effects of ozone dosage and initial concentrations of azo dyes. As a result, it could be concluded that both ozonation and UV/ozonation were very powerful for degradation of azo dyes. In addition, the decolorisation of diazo dyes was more difficult than monoazo dyes.

Ince (1997) realized drawbacks of textile dyeing and finishing wastewater treatment by conventional methods including biological, physical and chemical processes or their combinations, namely a number of refractory chemicals in the effluents and difficulty in the complete removal of color of common diazo dye, Remazol Black-B. The investigation was focused on monitoring the degradation and toxicity reaction of an aqueous solution of the dye up to 30 min of treatment by UV/H_2O_2 oxidation system. The dye was completely decolorized and converted to colorless intermediates, while only 44% of the organic carbon was mineralized. The influence of the initial H_2O_2 concentration on the rate of dye removal was important; however if H_2O_2 dose was too high, the degradation rate decreased. Nevertheless, it was important to note that the best operating conditions must be selected when real textile dyeing and finishing effluents, where large quantities of organic dyestuff, additives, non-ionic detergents and sulfates were present effects.

Chun and Yizhong (1999) investigated the photodegradation and biodegradability of non-biodegradable commercial azo dyes, Reactive YellowKD-3G, Reactive Red 15. Reactive Red 24, Cationic Blue X-GRL, an indicator, Methyl Orange, and one industrial wool textile wastewater. The photocatalytic reactions were carried out using TiO_2 suspensions irradiated with a medium pressure mercury lamp. The color removal of dyes, increasing of biochemical oxygen demand (BOD), decreasing of chemical oxygen demand (COD) and total organic carbon (TOC) were discussed. The biodegradability of the wastewater was explained in term of a ratio of BOD/COD, which was less than 0.3 in all selected azo dyes solution. It was, therefore, concluded that the azo dyes were difficult to be biodegraded.

Zamora *et al.* (1999) compared degradation of reactive dye (C.I. reactive blue-19) among ozonation, enzymatic and photochemical processes. For the ozonation process, decolorisation was very fast when the visible region was monitored using UV/VIS spectrophotometer, nevertheless, decomposition in the ultraviolet region was not observed. The decolorisation using enzymatic process was very slow. The best result was found for the photocatalytical process. The use of ZnO or TiO_2 as photocatalysts lead to decolorisation and mineralization of the dye, that the photodegradation using TiO_2 was more efficiency than using ZnO.

Review of various semiconductors used in photocatalytic degradation

Nogueira and Jardim (1993) studied photodegradation of Methylene Blue (MB) under solar light using three catalysts i.e. metal oxides (TiO_2, ZnO) and metal sulfides (CdS). It was found that TiO_2 was the best of the three catalysts.

Vinodgopal *et al.* (1994) decolorized two commercially used textile azo dyes, including Acid Orange 7 and Direct Blue 1, using colloidal TiO_2 and WO_3 photocatalytic systems. Under UV irradiation, these dyes underwent rapid decolorisation as they were reduced at the semiconductor surface by the trapped electrons. The quantum efficiency for such a reductive process had been determined to be 4.7%. The rate constant for the electron transfer between the excited semiconductor colloid and the dye was in the order of 10^8 $M^{-1}s^{-1}$. This photocatalytic decolorisation approach had potential applications in the treatment of textile dye wastes.

Nasr *et al.* (1996) utilized visible light to degrade the textile diazo dye, Naphthol Blue Black on TiO_2 semiconductor nanoparticles. The importance of semiconducting properties was further highlighted due to the failure of the dye to degrade on support material such as Al_2O_3 or in the absence of oxygen. The primary event following visible light excitation was the charge injection from the excited dye molecule into the conduction band of the semiconductor TiO_2, producing the dye cation radical. The surface adsorbed oxygen played an important role in scavenging photogenerated electrons, thus preventing the recombination between the dye cation radical and photoinjected electrons. Diffuse reflectance transient absorption and FTIR techniques were used to elucidate the mechanistic details and identify intermediates or end products of the dye degradation. The degradation was confirmed proceeding via the photosensitization pathway for these dyes. They also concluded that the degradation could be achieved for complete mineralization using broad band illumination that would combine the photocatalytic and photosensitized degradation.

Vinodgopal and Wynkoop (1996) investigated photosensitized degradation of textile azo dye, Acid Orange 7, on TiO_2 particles using visible light. They also confirmed the work reported by Nars *et al.*, (1996) that degradation did not occur on Al_2O_3 surface or in the absence of oxygen. The surface absorbed oxygen played an important role in scavenging photogenerated electrons, thus preventing the recombination between the oxidized dye radical and the photoinjected electrons. Diffuse reflectance FTIR was used to make an identification of reaction intermediates and end products of dyes. Though less explored in photocatalysis, the photosensitization approach could be an excellent choice for the degradation of colored pollutants using visible light.

Reutergårdh and Iangphasuk (1997) examined the photocatalytic degradation of Reactive Black 5 (RB5), a reactive azo dye, using TiO_2 and CdS as photocatalysts. An aerated semiconductor suspension was illuminated in a batch-lab-scale reactor. The UV light source (75W high pressure mercury lamp) was used in the case of TiO_2 photocatalysis, whereas the visible light source (100W Philips lamp) was used for CdS photocatalysis. Both reactions followed first order kinetics. The different light sources were used because they realized that TiO_2 could be activated only under UV light, whereas CdS could be excited under visible light such as sunlight. The effects of initial pH, semiconductor dosage, light intensity, initial dye concentration and temperature were investigated. The RB5 wastewater was decolorized and detoxified by TiO_2 photocatalysis. By contrast, CdS photocatalysis increased the toxicity due to CdS photocorrosion or photodissolution of Cd^{2+}. An important advantage of photocatalysis was photocatalysts could be recycled to reduce operational costs. It was found that the efficiencies of photocatalytic decolorisation using new and recycled TiO_2 were not significantly different. On the other hand, the reaction using recycled CdS was lower efficient than that for new CdS.

Bandara *et al.* (1999) studied disappearance of an azo dye, Orange II, in photocatalyzed processes on Fe, Ti and Al oxides under visible light irradiation. The detail of the charge injection from the excited state of Orange II into the catalyst, charge recombination and the rate between the dye and free hydroxy radical were reported by laser-pulsed spectroscopy. The intermediates generated on the oxide surface by the adsorbed azo dye during irradiation were identified by FTIR and in solution by HPLC. The rate of disappearance of Orange II was $Fe_2O_3 > TiO_2 > Al_2O_3$, respectively.

Xu and Langford (2001) examined photodegradation of a textile dye, Reactive Brilliant Red X3B using either UV (λ = 320 nm) or visible light (λ = 450 nm) over three catalysts of highly adsorptive TiO_2 nanoparticles in water. The common observation was confirmed that for all the reactions induced by UV or visible light, the apparent initial rate of X3B loss in the aqueous phase increased with the initial equilibrated concentration of X3B. However, this correlation was changed when the rate was determined by the decrease in concentration both in the aqueous phase and on the catalyst surface. This increase of real initial rate with the initial equilibrated concentration was observed only in the visible-light-induced reaction over TiO_2 of Degussa P25. For all the other reactions, especially under UV irradiation, the real initial rate was found to increase only initial and then decrease with the initial equilibrated concentration. The result suggested that there was a screening effect by the adsorbed dye in the TiO_2 photocatalytic reaction and a solution filter effect in the photosensitized reaction. Moreover, the photosensitized photodegradation of X3B was found to be also dependent on the physical properties of TiO_2, but interestingly the relative activity among the catalysts was similar to that demonstrated in the photocatalytic reaction.

Sakthivel *et al.* (2003) investigated the photocatalytic activity of commercial ZnO powder and compared with that of Degussa P25 TiO_2. Laboratory experiments with Acid Brown 14 as the model pollutant have been carried out to evaluate the performance of both ZnO and TiO_2 catalysts. Solar light was used as an energy source for the photocatalytic experiments. These catalysts were examined for surface area, particle size and crystallinity. The effects of initial dye concentration, catalyst loading, irradiation time, pH, adsorption of Acid Brown 14 on ZnO and TiO_2, intensity of light and comparison of photocatalytic activity with different commercial catalysts were studied. The progress of photocatalytic degradation of the Acid Brown 14 has been observed by monitoring the change in substrate concentration of the model compound employing HPLC and measuring the absorbance in UV–VIS spectrophotometer for decolorisation. The photodegradation rate was determined for each experiment and the highest value was observed for ZnO suggesting that it absorbed large fraction of the solar spectrum and absorption of more light quanta than TiO_2. The complete mineralization was confirmed by total organic carbon (TOC) analysis, COD measurement and estimation of the formation of inorganic ions such as NH_4^+, NO_3^-, Cl^- and SO_4^{2-}.

Review of various noble metals deposited on TiO_2

Bamwenda *et al.* (1995) compared the photocatalytic activity for H_2 generation between Au/TiO_2 and Pt/TiO_2 in two reactions of C_2H_5OH as shown Eqs. (i) and (ii)

$$C_2H_5OH + H_2O \xrightarrow[\text{photocatalyst}]{h\nu} 2H_2 + CH_4 + CO_2 \quad \text{(i)}$$

$$C_2H_5OH + H_2O \xrightarrow[\text{photocatalyst}]{h\nu} 2H_2 + CH_4 + CO_2 \quad \text{(ii)}$$

The deposition of Au and Pt was carried out using TiO_2 powder in aqueous suspensions containing $HAuCl_4.4H_2O$ or $H_2PtCl_6.6H_2O$ by deposition-precipitation (DP), impregnation (IMP), photodeposition (FD) and in the case of Au, by mixing TiO_2 with colloidal gold suspension (MIX). The main reaction products obtained from the irradiation of an aqueous 5M C_2H_5OH suspension containing Au/TiO_2 or Pt/TiO_2 were hydrogen, methane, carbon dioxide, acetaldehyde and small amounts of acetic acid. The activity of Au samples was generally about 30% lower than that of Pt samples. The activity of Au samples strongly depended on the preparation method and decreased in the order of FD>DP>IMP>MIX, while the activity of Pt samples was less sensitive to the preparation method and decreased in the order FD>DP≈IMP. The activities for H_2 generation of Au and Pt decreased with increasing calcinations temperature, the highest activity was shown at 573 K. The H_2 generation was found to be dependent on the metal content on TiO_2 and showed a maximum in the range 0.3-1 wt% of Pt and 1-2 wt% of Au. Moreover, the rate of H_2 production was strongly dependent on the initial pH of the suspension, pH values in the range 4-7 gave better yields, whereas highly acidic and basic suspensions resulted in a considerable decreased in the H_2 yield.

Li, F. B. and X. Z. Li (2002) studied gold/gold ion on TiO_2 to improve photocatalytic properties for wastewater treatment. The gold ion-doped TiO_2 was prepared by the sol-gel method while the gold-deposited TiO_2 was prepared by the photoreduction method. The photoactivity was quantified by degradation of Methylene Blue (MB) and formation of the reaction products NH_4^+, NO_3^- and SO_4^{2-}. The aqueous suspensions containing MB and catalyst were magnetically stirred in dark condition for 15 min, and then they were irradiated under UV light (High Pressure mercury lamp) with constant aeration. The results showed that the presence of gold ion/gold on TiO_2 surface greatly enhanced their photoactivity, and the optimal molar content of gold ion doping and gold deposition was 0.5%. The enhancement of photoactivity due to the presence of gold or gold ion was confirmed using i) X-ray photoelectron spectroscopy showed that the species of Au, Au^+, Au^{3+} and Ti^{3+} existed in/on TiO_2 which affected the properties of catalysts such as recombination of-hole pairs ii) photoluminescence (PL) spectroscopy showed that the PL intensity decreased and iii) light absorption of the modified TiO_2 catalysts shifted to longer wavelength, which was lower than the band gap of TiO_2 (3.2 eV).

Arabatzis *et al.* (2003) attempted to enhance the decomposition reaction rate of industrial water pollutants by gold deposition via electron beam evaporation, which surface was modified including rough, high-surface area, nanocrystalline titania thin film photocatalysts. The materials were characterized and their photocatalytic activity was tested for Methyl Orange photodegradation. All solutions were O_2-bubbled for 2 h, and then were irradiated using four parallel 15W blacklight tubes (maximum emission at 350 nm) under magnetic stirring. The optimal concentration of gold particles was found to be 0.8 $\mu g\ cm^{-2}$, and remained stable after several photocatalytic cycles of new added pollutant as well. However, higher surface loadings decreased the efficiency, and this can be understood in terms of an optimum gold particle size and surface characteristics as well as the semiconductor availability for light absorption and pollutant adsorption. The results showed that Au/TiO_2 photocatalyst at the optimal concentration leaded to a two times faster degradation with respect to the rate obtained with the original TiO_2 material. This enhancement was attributed to the action of Au particles, which played a key role by attracting conduction band photoelectrons and preventing electron-hole recombination.

Subramanian *et al.* (2003) synthesized gold-capped TiO_2 nanocomposite particles by reducing $[AuCl_4]^-$ on the surface of TiO_2 colloids in acetonitrile with $NaBH_4$. Such semiconductor metal nanocomposites were considered to be beneficial toward improving the efficiency of the photocatalytic oxidation process. They compared the absorption properties of Au/TiO_2 prepared by a chemical reduction method with that of the photocatalytic method. The surfaced adsorbed $AuCl_4^-$ captured the photogenerated electrons and were reduced at the interface, they expected the reduction of Au(III) to Au^0 to occur in sequential steps, Au(III)→Au(II)→Au(I)→Au^0. In addition, they prepared photocatalyst samples from UV irradiated suspensions of TiO_2 and $AuCl_4^-$ in deaerated acetonitrile to answer that how the ratio of $[Au^0]/[Au^{(III)}]$ at the TiO_2 interface influenced the net photocatalytic efficiency. A known amount of thiocyanate was added and the formation of $(SCN)_2^{\cdot -}$ yield was measured in a laser flash photolysis experiment. The presence of both Au(III) and Au^0 at the TiO_2 interface were beneficial at low concentration levels.

Zanella *et al.* (2004) prepared Au/TiO_2 catalysts by two methods, deposition-precipitation with NaOH (~ 3 wt% Au) and with urea (~ 8 wt% Au). The different amount of the gold loading was due to all the gold from the solution was deposited on TiO_2 only in the case of urea. These catalysts were also calcined at various temperatures (100, 200, 300 and 400 °C). The particle size increased from 1.5 to 3.5 nm with the calcination temperature. The photocatalytic activity which was tested in the reaction of CO oxidation was maximum after calcination at 200 °C for both types of samples, while the activity dropped at higher temperature.

Sakthivel *et al.* (2004) studied enhancement of photocatalytic activity by metal deposited on TiO_2 catalysts. The studied metals consisted of Pt, Au and Pd which were prepared easily by impregnation method. They were characterized by surface analytical methods such as surface area, XRD and scanning electron micrograph and photophysical characterization by diffuse reflectance spectroscopy. The photocatalytic activity of doped catalyst was evaluated by degradation and decolorisation of leather dye, Acid Green 16, in aqueous solution illuminated with low pressure mercury lamp (254 nm). The efficiencies of Pt, Au and Pd deposited TiO_2 were compared with that of TiO_2. They found that Pt deposited TiO_2 was almost comparable to Au/TiO_2 but higher than Pd/TiO_2. In addition, the efficiency increased with increasing in the metal loading up to an optimum level due to the effect of decreasing recombination of electron and hole. Above the optimum metal doping, the dopants behaved as electron-hole recombination centers and hence lower photonic efficiency.

Review of photocatalytic degradation of dyes

Davis *et al.* (1994) studied the photocatalytic decolorisation of municipal wastewater contaminated with textile dyes using a batch reactor. Degussa P25 TiO_2 was used as the photocatalyst and proved efficiency for dye degradation when irradiated with UV light in the presence of air. In addition, the photocatalytic reaction simultaneously reduced the COD which suggested that the dissolved organic compounds have been oxidized, thereby removal the color of the wastewater. The activation energy for the photocatalytic decolorisation reaction was only about 3 to 6 kJ/mole. These result suggested that the photocatalytic degradation of textile dyes may be a viable method for decolorizing and oxidizing organic compounds in wastewater.

Tang and An (1995) studied kinetics of photocatalytic oxidation of five commercial dyes in a TiO_2/UV slurry reactor. They concluded that oxidation kinetics of dyes strongly depended upon the molecular structures of their chromophore and followed the L-H model at all studied pH values for Direct Blue 160 and Reactive Red 120 but the kinetics of Acid Blue 40, Basic Yellow 15 and Direct Blue 87 followed L-H model at different pH. At low pH, reduction by electrons in conduction band may be a very important role in the degradation of azo dyes due to the reduction cleavage of azo bond. The oxidation rates followed in the decreasing order: monoazo dye of Basic Yellow 15 > diazo dye of Reactive Red 120 > triazo dye of Direct Blue 160. At neutral or high pH, hydroxyl radical ($^{\bullet}OH$) may be the predominant oxidation species.

Sangchakr *et al.* (1995) studied photocatalytic degradation of sodium benzene sulfonate and its substituted compounds. The experiment was carried out under 500W super high pressure mercury lamp in TiO_2 suspension. The formation of SO_4^{2-}, H^+ and CO_2 and elimination of TOC were determined. After 5 h of illumination, the concentration of SO_4^{2-} was closed to the amount of sulfur contained in the initial solution. They also identified one major and two minor intermediate products; p-phenolsulfonic acid, hydroquinone and p-quinone. In addition, the degradation rates of several p-substituted benzenesulfonates were compared to estimate the effect of the substituent group, that is, electron-donating substituents accelerated the degradation rate while electron-accepting substituents retarded the rate.

Tang *et al.* (1997) studied kinetics of photocatalytic degradation of eleven azo dyes using TiO_2/UV. They suggested that both hydroxyl radicals and positive holes played an important role in the degradation of the commercial dyes depending upon their molecular structures. The degradation kinetics of azo dyes seems to be significantly influenced by their electrical nature, the number of azo bonds present in a dye molecule, and type of auxiliary groups attached to the azo bonds such as the number of naphthalene group. The order of the difficult to degrade were triazo dyes, diazo dyes and monoazo dyes, respectively. A Rayonet photochemical reactor equipped with 16 UV lamps inside a chamber was used for photocatalytic oxidation reactions. TiO_2/UV photocatalytic degradation of azo dyes is also affected by pH. The pH effects on the degradation kinetics of different dyes may be due to the intrinsic reactivity of the neutral and ionized dye species at various pH levels towards positive hole oxidation or hydroxyl radical attack.

Kiriakidou *et al.* (1999) investigated photocatalytic degradation over TiO_2 irradiated under a light source simulating solar light of Acid Orange 7 (AO7), a non-biodegradable azo-dye. When only visible light is used (>400 nm), degradation of AO7 was low but appreciable rate suggested that the mechanism involving photosensitized electron injection leading to charge separation with light of less than band energy. The effect of operational parameters, i.e., dye concentration, photocatalyst content, pH of the solution and incident light energy on the degradation rate of aqueous solutions of AO7 was examined. Cation doping of TiO_2 for the development of photocatalysts with improved efficiency were investigated with valence higher (W^{6+}) and lower (Ca^{2+}) than the parent cation (Ti^{4+}) in the TiO_2 matrix. Results showed that the employment of efficient photocatalysts and the selection of optimal operational parameters may lead to complete decolorisation and to substantial decrease of the Chemical Oxygen Demand of the dye solutions.

Galindo *et al.* (2000) showed the results obtained from the oxidation of the aminoazobenzene dye AO52 by the UV/H_2O_2, UV/TiO_2 and VIS/TiO_2 systems. Both UV/H_2O_2 and UV/TiO_2 can be efficiently used. Although the VIS/TiO_2 seemed to be less effective, the capability could be improved by combining UV and visible irradiations, i.e. using non-expensive sunlight. They investigated the formation of first by-products using GC/MS, HPLC and ^1H NMR. In this paper, they described degradation mechanism, however its mechanism has not yet been completely classified. Besides, degradation by the UV/TiO_2 system was pH dependent.

Tanaka *et al.* (2000) studied photodegradation of seven azo dyes in TiO_2 suspension under illumination by a 500 W superhigh pressure mercury lamp. Their degradation rates were compared with disappearance and TOC elimination rates. Major intermediates identified were aromatic amine, phenolic compounds and several organic acids. It was indicated from their study that in the photocatalytic degradation of azo dyes proceeded through both oxidation and reduction, whereas TOC was eliminated predominantly by oxidation. They concluded that i) in photocatalytic degradation of azo dyes, diazo dye was less degradable than monoazo, ii) the order of photocatalytic degradation rates approximated to ozonation process cited from literature, iii) adsorption of dye to TiO_2 was one of the important factors determining the degradation rate and iv) photocatalytic degradation of azo dye proceeds predominantly through oxidation by positive hole (or $^{\bullet}OH$) and reduction by conduction band electron.

Neppolian *et al.* (2002) utilized solar light to treat hazardous and toxic of textile wastewater. Aqueous solutions of Reactive Blue 4 textile dye was mineralized when irradiated with TiO_2 photocatalyst. A solution containing 4×10^{-4} M dye was completely degraded in 24 h irradiation time. The intensity of the solar light was measured using Lux meter. The results showed that the dye molecules were completely degraded to CO_2, SO_4^{2-} , NO_3^-, NH_4^+ and H_2O under solar irradiation. The addition of hydrogen peroxide and potassium persulphate influenced the photodegradation efficiency. The rapidity of photodegradation of dye intermediates were observed in the presence of hydrogen peroxide than in its absence. The auxiliary chemicals such as sodium carbonate and sodium chloride substantially affected the photodegradation efficiency. High performance liquid chromatography and chemical oxygen demand were used to study the mineralization and degradation of the dye respectively. It was concluded that solar light induced degradation of textile dye in wastewater is a viable technique for wastewater treatment.

Augugliaro *et al.* (2002) reported the photodegradation of two common and very stable azo-dyes, i.e. Methyl Orange ($C_{14}H_{14}N_3SO_3Na$) and Orange II ($C_{16}H_{11}N_2SO_4Na$). The photocatalytic oxidation was carried out in aqueous suspensions of polycrystalline TiO_2 irradiated by sunlight. The disappearance of color and substrates together with the abatement of total organic carbon content was monitored. The main sulfonate-containing intermediates were found to be in lower number with respect to those obtained under artificial irradiation. In particular there was no more evidence of the presence of hydroxylated transients. The dependence of dye photooxidation rate on: i) substrate concentration; ii) catalyst amount; and iii) initial pH were investigated. The influence of the presence of strong oxidant species (H_2O_2, $S_2O_8^{2-}$) and some ions (Cl^-, SO_4^{2-}) on the process was also studied.

Baiocchi *et al.* (2002) successfully applied HPLC/UV-VIS diode array and HPLC/MS techniques to analysis of sulfonated molecules present in samples coming from the photocatalytic degradation of the azo dye indicator, Methyl Orange (MO). TiO_2 P25 was used as photocatalyst. Aqueous TiO_2 dispersions containing MO was irradiated using 1500W Xe-arc lamp to produce a simulated sunlight under aerobic conditions. The degradation of MO during the irradiation was monitored together with the formation of the inorganic final products (SO_4^{2-}, NO_3^-, NH_4^+) and the TOC evolution. The obtained results confirmed that HPLC-MS was a suitable technique. The structural information about the degradation intermediates achieved from MS and MS/MS studies were quite compatible with the photocatalytic degradation steps.

Lachheb *et al.* (2002) investigated the photocatalytic degradation of five various dyes in TiO_2/UV aqueous suspension. It was attempted to determine the feasibility of such degradation by varying the chemical structures, either anthraquinonic (Alizarin S (AS)), or azoic (Crocein Orange G (OG), Methyl Red (MR), Congo Red (CR)) or heteropolyaromatic (Methylene Blue (MB)). In addition to a prompt removal of the colors, TiO_2/UV based photocatalysis was able to fully oxidize the dyes, with a complete mineralization of carbon into CO_2 and Sulfur was converted into SO_4^{2-}. The mineralization of nitrogen was more complex. Nitrogen atoms in the −3 oxidation state, such as in amino groups, remain at this reduction degree and produced NH_4^+ cations, subsequently and very slowly converted into NO_3^- ions. For azo dye (OG, MR, CR) degradation, the complete mass balance in nitrogen indicated that the central –N=N– azo group was converted in gaseous dinitrogen, which is the ideal issue for the elimination of nitrogen containing pollutants, not only for environmental photocatalysis, but also for any physicochemical method. The aromatic rings were submitted to successive attacks by photogenerated $^{\bullet}OH$ leading to hydroxylated metabolites before the ring opening and the final evolution of CO_2 occurred. These results suggest that TiO_2/UV photocatalysis may be envisaged as a method for treatment of diluted colored wastewaters not only for decolorisation, but also for detoxification, in particular in textile industries in semi-arid countries.

Saquib and Muneer (2003) investigated photocatalytic degradation of a triphenylmethane dye (Gentian Violet) in aqueous suspensions of TiO_2 under UV light and oxygen. They studied degradation by monitoring the change in substrate concentration and decreased in total organic carbon content as a function of irradiate time. The degradation of dye was studied under a variety of conditions such as pH, catalyst concentration, substrate concentration, different types of TiO_2 and in the presence of electron acceptors such as hydrogen peroxide (H_2O_2) and ammonium persulphate $(NH_4)_2S_2O_8$. The photocatalyst Degussa P25 was found to be more efficient as compared with other photocatalysts (PC500 and UV100). The degradation products were analyzed by GC/MS technique and pathways for the formation of the products were proposed.

Silva and Faria (2003) investigated the photochemical and photocatalytic degradation of aqueous solutions of an azo dye, Solophynyl Green (SG) BLE 155%, by UV irradiation. Direct UV irradiation demonstrated to be very efficient for low initial concentrations of dye. For higher concentrations the photocatalytic degradation was carried on TiO_2, and this semiconductor was mixed with different activated carbons (AC). The kinetics of photocatalytic degradation were found to follow a first-order rate law. It was also observed that the presence of the activated carbon enhanced the photoefficiency of the TiO_2 photocatalyst.

Stylidi *et al.* (2003) studied the use of a solar light simulating source (450W Xe-arc lamp) to degrade aqueous solutions of Acid Orange 7 in TiO_2 (P25) suspensions. The photoreaction was followed by monitoring the degradation of the dye and the formation of intermediates and final products, as functions of time of irradiation, both in solution and on the photocatalyst surface with a variety of techniques. It has been found that the dye adsorbs on TiO_2 and undergoes a series of oxidation steps, which lead to decolorisation and formation of a number of intermediates, mainly aromatic and aliphatic acids. These molecules are further oxidized toward compounds of progressively lower molecular weight and, eventually, to CO_2 and inorganic ions, such as sulfate, nitrate and ammonium ions. A TiO_2-mediated photodegradation mechanism for Acid Orange is proposed on the basis of quantitative and qualitative detection of intermediate compounds.

Guillard *et al.* (2003) degraded anionic (Alizarin S (AS), azo-Methyl Red (MR), Congo Red (CR), Orange G (OG)) and cationic (Methylene Blue (MB)) dyes either individually or in mixtures using UV irradiated TiO_2 in suspension or supported on glass and on paper. The influence of the chemical structure of different dyes as well as that of pH and of the presence of inorganic salts on the photocatalytic properties of TiO_2 has been discussed. The role of adsorption is suggested, indicating that the reaction occurs at the TiO_2 surface and not in the solution. S and N atoms are respectively mineralized into SO_4^{2-}, NO_3^- and NH_4^+, except azo groups which mainly formed N_2 which represents an ideal case for a decontamination reaction. The fate of nitrogen strongly depends on its initial oxidation degree. High photocatalytic activities have been found for TiO_2 coated on glass by the sol–gel method. Its efficiency was intermediate between those of PC500 and P25 powders. The efficiency of PC500 TiO_2 sample, fixed on paper using a binder, is slightly less important than that of the powder. The presence of a silica-binder is suggested to be at the origin of the decrease in efficiency.

Qamar *et al.* (2005) selected two dye derivatives, Chromotrope 2B (1) and Amido Black 10B (2), and then investigated them in aqueous suspensions of TiO_2 in the presence of light and oxygen. The experiments were done under a variety of conditions to obtain a high degradation rate, which depended strongly on the kind of pollutant. The photocatalytic degradation was monitored by measuring the change in substrate concentration as a function of irradiation time employing UV spectrophotometry. A number of byproducts were formed during the photooxidation process which were potentially harmful to the environment, therefore, investigators have studied the mineralization of the pollutants by measuring the total organic carbon (TOC). The degradation of dyes were studied using different parameters such as types of TiO_2, pH, catalyst concentration, substrate concentration and in the presence of different acceptors such as H_2O_2, $KBrO_3$ and $(NH_4)_2S_2O_8$ besides molecular oxygen. The degradation rates were found to be strongly influenced by all above parameters. The photocatalyst Degussa P25 was found to be more efficient as compared with other photocatalysts. Investigators found the degradation of dye derivative (1), monoazo dye, was faster than the dye derivative (2), which was diazo dye.

MATERIALS AND METHODS

Materials

1. Apparatus

The apparatus employed in the photocatalytic experiments consisted of the research arc source (Oriel, model 69907, USA). The light source was furnished with solar-light simulating Xe-arc lamp (150 W Xenon, ozone free, model: 6255, 0.5 x 2.2 mm), approximate flux and brightness of this lamp were 300 lumens and 3,000 cd/mm^2, respectively. For the experiments, the lamp power was kept constant at 150 W, the photoreactor was placed at a fixed distance of 25 cm. from the lamp housing. Experiments were performed at room temperature.

The photoreactor was setup as shown in Figure 2. The solution was carried out in the beaker as well as covered by the box to protect extraneous light.

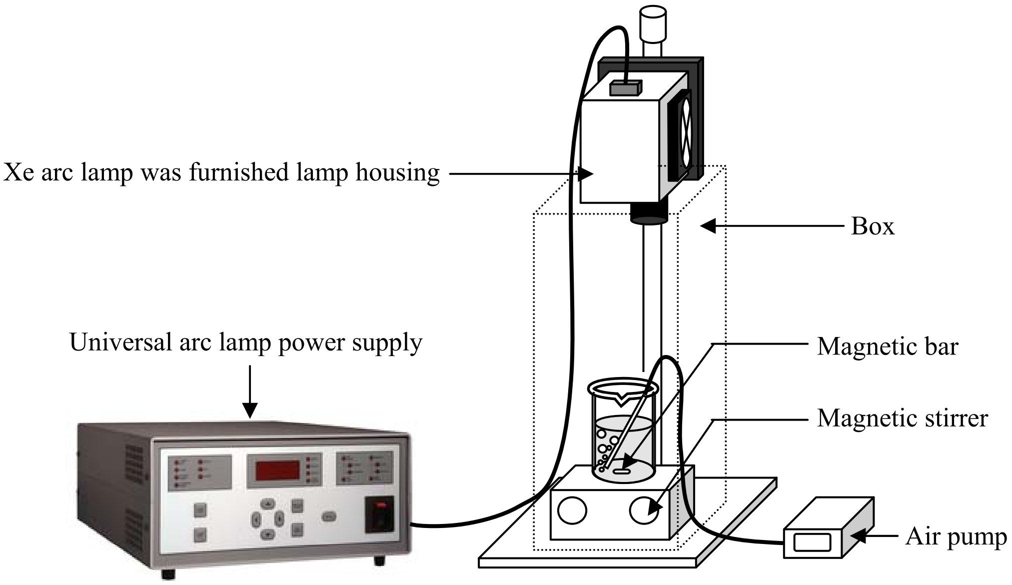

Figure 2 Schematic of solar-light simulating photoreactor

Ultra-pure water was prepared using water purification system, Simplicity (Millipore, France).

The solution was stirred with magnetic stirrer (Heidolph model MR3000, Germany) and bubbled with an air pump (Boyo, SC-7500, Thailand).

The pH measurements were made on Corning model 430 pH meter (USA).

Hettich zentrifugen Universal 32R (Germany) was used for gathering prepared catalyst and ADAMS compact II (USA) was used to centrifuge and separate the suspended solutions.

Bondelin Sonosex TK52 (USA) and Cole-Parmer® model 08849-2 cleaner ultrasonic bath were used for degassing a mobile phase and dissolving the sample solution.

Lux/FC light meter, Tenmars model DL-204 purchased from Worldwide Trade Thai Co., Ltd., Thailand was used to measure the intensity of light.

Absorbance changes caused by irradiation were monitored with PerkinElmer model Lambda 35 UV/VIS spectrometer (USA) in 1 cm quartz cell.

The detection of loaded gold on the TiO_2 was carried out by graphite furnace/zeeman atomic absorption spectroscopy (Varian, SpectraAA 880Z, USA) and gold/TiO_2 surface was analyzed by the scanning electron microscopy (SEM), model 145 OVP (Leo).

The intermediates formed during the degradation process were identified by LC/DAD, LC/MS/MS and Ion Chromatography instrument.

1.1 LC/DAD system

The LC/DAD analysis was performed on the Varian ProStar liquid chromatograph, USA, equipped with a ProStar 230 solvent delivery pump, Rheodyne model 7725i six-port valve with a 20 µL sample loop and ProStar 330 photodiode array detector operated in the range of 190-400 nm. The system was controlled by Star workstation software. The separation was carried on LiChrospher®60 RP-select B column (250 mm x 4.6 mm I.D., 5 µm, Merck, USA).

1.2 LC/MS/MS system

The LC/MS/MS analysis consisted of LC system and tandem mass spectrometry. LC system equipped with Agilent 1100 Series, USA, binary pump and Rheodyne model 7725i six-port value with 20 µL sample loop. The separation was carried on LiChrospher®60 RP-select B column (250 mm x 4.6 mm I.D., 5 µm, Merck, USA). Tandem mass spectrometry was performed on a triple-quadrupole mass spectrometer PE ScieX model API 2000 (Applied Biosystems) equipped with atmospheric pressure chemical ionization (APCI) interface. Mass calibration of resolving quadrupoles was carried out by continuous infusion of a solution of polypropylene glycols (PPGs) via the system's built-in infusion pump. Nitrogen was used as collision gas. Analyst 1.1 Software was used for data acquisition and data analysis. Nitrogen (99.998%) was used for nebulizer and collision gas.

1.3 Ion Chromatography

The ion chromatography instrument was a Dionex Model DX-500 (USA), equipped with a GP40 gradient pump, and an ED40 conductivity detector with Anion Self - Regenerating Suppressor (ASRS_2mm) suppression. Dionex IonPac® AS17 (250 mm x 2 mm) analytical column packed with anion-exchange resin was used. Other conditions were a 10 µL sample loop, suppressor current of 19 mA, column temperature of 30 °C and pump flow rate of 0.25 mL/min. Data acquisition and instrument control were performed using the Chromeleon Chromatography Information Management System.

A Dionex EG40 eluent generator equipped with an EGC-KOH cartridge was used. The EGC-KOH cartridge was placed between the pump outlet and the EG40 degas assembly inlet. The degas assembly outlet was connected to the sample injection.

2. Reagent

Powdered TiO_2 was purchased from Carlo Erba (analytical grade reagent), its purity is more than 98.5%. Tetrachloroauric (III) acid ($HAuCl_4.3H_2O$) in 12.7% iger salzsaure solution was purchased from Merck, USA. It was used throughout the experiments. TiO_2 was used as a standard photocatalyst, while gold was the noble metal doped on photocatalytic semiconductor surface.

Trypan Blue was purchased from Aldrich. Its characteristics were shown in Table 1.

Table 1 The characteristics of the Trypan Blue or Direct Blue 14

Type	Formular	Molecular Weight (g/mol)	Water solubility	Melting Point (°C)
Direct Dye	$C_{34}H_{24}N_6Na_4O_{14}S_4$	960.79448	0.1-1 g/100 mL at 20 °C	> 300

HPLC-grade acetonitrile and methanol were purchased from Merck. Ultra-pure water was used to prepare the LC and IC eluent.

Stock solution of individual standard was prepared at a concentration of 500 and 1000 mg/L. All other chemicals and reagents were analytical grade as listed in Appendix 1. DI water and Ultra-pure water were used throughout the experiments.

Methods

1. Preparation of gold deposited on TiO_2

Gold doped TiO_2 was prepared into two steps by first deposition and then reduction. In a deposition step, TiO_2 was dispersed in 10 mL of aqueous 0.42 M urea by the ultrasonic agitation for 30 min. Following, aqueous solution containing the required amount of gold dissolved in 0.42 M urea was added to the colloidal TiO_2 suspension. The ratio of the content of aqueous solution to the amount of TiO_2 powder was 100 mL : 0.5 g. The initial pH was about 2. This suspension was stirred vigorously and thermostated at 80 °C for 3 h to allow adsorption of negative charge of $[AuCl_4]^-$ ions on the positive charge surface of TiO_2 nanoparticles. Urea deposition leaded to a gradual rise in pH from 2 to 8, and the color change of solution was from yellow to colorless as well. Furthermore, the pH value of colloidal gold/TiO_2 suspension was adjusted to 3 by dropwise addition of CH_3COOH. The acidic value of suspension was required as the electrostatic attraction of the positive change on TiO_2 surface with negative charge of $[AuCl_4^-]$ ions leaded to enhancement of the adsorption (Wang *et al.,* 1997).

Reduction of the $[AuCl_4]^-$ was achieved by the dropwise addition of solution of $NaBH_4$ (10 mM acetonitrile) in the gold/TiO_2 suspension, to ensure the complete reduction of Au(III) to Au^0 (Dawson and Kamat, 2001 and Subramanian *et al.,* 2003). Figure.3 shows the principle of preparation of the gold/TiO_2 nanoparticles (Mallick *et al.,* 2004). The gold/TiO_2 precipitate changed from white to pink, while in the case of more and more gold the color would change from white to pink and continued to purple. The $NaBH_4$ solution was dropped until no color change was observed. The solids were gathered by centrifugation (6,000 rpm for 15 min). After centrifugation, a colorless filtrate was kept to evaluate residual gold. The prepared catalysts were washed in 50 mL of ultra pure water under stirring for 10 min at 50 °C, and then they were separated by centrifugation. The operation for washing of catalysts was repeated four times. The catalysts were dried under vacuum in the desiccator at room temperature for 10 h or at 100 °C for 2 h. Then, the dried catalysts were calcined for 4 h at various temperature (Zanella *et al.*, 2004).

The above procedure was used for the preparation of Au/TiO_2 at 0.1, 0.5, 1.0, 1.5, and 2.0 % gold loading, then calcined at 400 °C for 4 h.

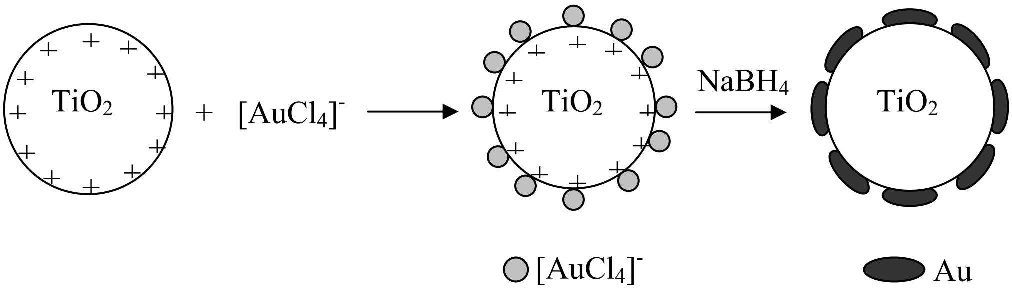

Figure 3 Adsorption and reduction of $[AuCl_4]^-$ ions on the TiO_2 surface

2. Characterization of gold / TiO_2

Detailed surface image was carried by means of a scanning electron microscope (SEM). Carbon coated sample has been performed to avoid problem arising from surface charge effected. The result is shown in Figure 5.

The amount of gold was evaluated using graphite furnace/Zeeman atomic absorption spectrometer. One gram of the catalyst gold/TiO_2 was digested in 10 mL beaker with 1 mL of HCl : HNO_3 (3 : 1) at 80 °C for 1 h. Blank was prepared in the same manner. All samples and blank were filtered through 110 mm Whatman No.42 and transferred to 10 mL volumetric flask, then diluted with DI water.

In addition, the colorless filtrates obtained from the gold/TiO_2 preparation were evaporated and diluted to 25 mL.

The calibration graph of gold was prepared in range over 0 to 40.0 ppb as shown in Figure 6. The preparation of gold solution was made by diluting the 1000 ppm gold stock solution with 0.5% HNO_3 in DI water. The peak area measurement was monitored at wavelength, slit width and lamp current of 242.8 nm, 1.0 nm and 10.0 mA, respectively. The operating parameters were carried out under the conditions given in Table 2. The result is shown in Table 11.

Table 2 Instrumental parameters for the graphite furnace AA spectrometer

Step No.	Temp (°C)	Time (sec)	Gas Flow (L/min)
1	85	5.0	3.0
2	95	40.0	3.0
3	120	10.0	3.0
4	500	5.0	3.0
5	500	1.0	3.0
6	500	2.0	0.0
7	2600	1.2	0.0
8	2600	2.0	0.0
9	2600	2.0	3.0

3. Photodegradation experiments

The photocatalytic efficiencies of gold/TiO_2 catalysts were evaluated using an aqueous solution of Trypan Blue as a model of pollutant. The various parameters consist of gold loading, calcination temperature, initial pH of aqueous Trypan Blue, concentration of Trypan Blue and gold/TiO_2 dosage were studied.

3.1 Effect of gold loading on TiO_2 on photodegradation of Trypan Blue

Five milligrams of photocatalysts with various gold loading, 0.1 – 2.0 wt%, calcined at 400 °C were added to 8 mL of the aqueous Trypan Blue solutions, which was fixed at 5.20×10^{-5} M (corresponding to 50 mg/L), pH values of 7 (natural) in test tubes. The experiment with TiO_2 without gold loading was also performed.

The procedures used for the reactions were carried out under solar-light simulating photoreactor. Prior to photooxidation, the suspension was sonicated in dark condition for 30 min to disperse catalysts, and then magnetically stirred and air bubbled for 20 min in dark condition to establish an adsorption/desorption equilibrium condition. The position of tube was fixed to avoid the difference of light intensity. All aqueous solutions were immediately centrifuged (ADAMS compact II) at approximately 3,200 rpm for 10 min. The clear filtrate was taken and analyzed using UV/VIS spectrometer. After monitoring, they were gathered together with catalysts and irradiated again. The aqueous suspensions containing Trypan Blue and catalyst were repeated at required time intervals to monitor absorbance change. The results are shown in Figure 9 – 11 and Table 12.

3.2 Effect of calcination temperature on photodegradation of Trypan Blue

The temperatures of calcination were varied from 200 to 600 °C using the photocatalyst of 0.36 wt% gold/TiO_2. The dosage of photocatalyst fixed at 2.5 mg was added to 8 mL of 2.60 x 10^{-5} M (corresponding to 25 mg/L) of Trypan Blue at pH 7. The experiment was carried out as described in section 3.1. The results are shown in Figure 12-14 and Table 13.

3.3 Effect of initial pH of an aqueous Trypan Blue on photodegradation of Trypan Blue

Solutions containing 2.08 x 10^{-5} M of Trypan Blue were prepared at pH values of 3, 5, 7, 9 and 11, respectively. The pH value of solution was adjusted to required value using dilute NaOH and HNO_3. The 2.5 mg of 0.36 wt% gold/TiO_2, calcined at 400 °C was added to 8 mL Trypan Blue. The experiment was carried out as described in section 3.1. The results are shown in Figure 15 – 17 and Table 14.

3.4 Effect of dosage of gold/TiO_2 on photodegradation of Trypan Blue

The dosages of gold/TiO_2 (0.36 wt%, calcined at 400 °C) were varied in the range of 0.20 to 1.25 g/L. Solution containing 5.20 x 10^{-5} M of Trypan Blue (8 mL, at pH 7) was used. The experiment was carried out as described in section 3.1. The results are shown in Figure 18 – 20 and Table 15.

3.5 Effect of concentration of Trypan Blue on photodegradation of Trypan Blue

The concentrations of Trypan Blue were prepared to 2.08 x10^{-5}, 2.60 x 10^{-5} and 5.20 x 10^{-5} M (corresponding to 20, 25 and 50 mg/L, respectively). Solution containing 8 mL of aqueous Trypan Blue at pH 7 in the presence of 0.36 wt% gold/TiO_2, calcined at 400 °C was proceeded. The experiment was carried out as described in section 3.1. The results are shown in Figure 21 and Table 16.

4. Kinetic and intermediate analysis

The reaction suspension was prepared by adding 1.0 g/L of 0.36 wt% gold/TiO_2 calcined at 400 °C into 100 mL of 5.20 x 10^{-5} M (corresponding to 50 mg/L) of Trypan Blue, and pH value of 7 (natural). Onother experiments, 5.0 g/L of gold/TiO_2 was added into 100 mL and 250 mL of 2.60 x 10^{-4} M (corresponding to 250 mg/L) of Trypan Blue. The procedures were carried out under solar-light simulating photoreactor. Prior to photooxidation, the suspension was sonicated in dark condition for 30 min, and then magnetically stirred and air bubbled for 20 min in dark condition. At specific time intervals, 5 mL of degraded solution was collected and centrifuged for 10 min to remove photocatalysts, then filtered through a 0.45 μm membrane filters (Sartorius). The degraded solutions were analyzed as required.

Reaction decolorisation was measured using UV/VIS spectrometer for monitoring of absorbance change and study of the kinetic reaction. Study of kinetic reaction was evaluated at the maximum wavelength. The degradation products or intermediates were identified by three techniques consisted of LC with UV detection, LC with MS/MS detection and Ion Chromatography.

4.1 LC/DAD experiments

The column was LiChrospher®60 RP-select B column and the analytes were eluted with 5 mM ammonium acetate/acetonitrile at a flow rate of 1.0 mL/min. The mobile phase components were filtered through 0.2 μm membrane filters (Schleicher and Schuell, Germany) and degassed for 30 min in an ultrasonic bath before using. The absorption of degradation products was obtained by scanning wavelengths in the range of 190-400 nm and also monitored at 210, 238, 280, 316 and 380 nm. Equilibration time was 20 min. Gradient mobile phase program for LC/DAD analysis of Trypan Blue and Trypan Blue spiked in wastewater are shown in Table 3 and 4, respectively.

Table 3 Gradient mobile phase program for LC/DAD analysis of Trypan Blue

Time (min)	Flow rate (mL/min)	Acetonitrile (%)	Water (%)
0	1.0	0	100
2.50	1.0	0	100
3.00	1.0	20	80
5.50	1.0	20	80
10.00	1.0	80	20
12.00	1.0	90	10
17.00	1.0	90	10

Table 4 Gradient mobile phase program for LC/DAD analysis of Trypan Blue spiked in wastewater

Time (min)	Flow rate (mL/min)	Acetonitrile (%)	Water (%)
0	1.0	25	75
5.50	1.0	25	75
6.00	1.0	50	50
10.00	1.0	10	90

4.2 APCI-MS/MS spectrometric analysis

4.2.1 Continuous flow infusion experiments

Q1 scan mass spectrum of each compound was recorded in both positive (PI) and negative ionization (NI) modes with scan range between m/z 100 and 950 amu, multi component analysis (MCA) 10 cycles, dwell time 1 sec. The specific precursor ion was selected from Q1 scan mass spectrum corresponding to the protonated molecular ion $[M + H]^+$ in PI mode and deprotonated molecular ion $[M – H]^-$ in NI mode. Then, product ion scan mass spectrum of each precursor ion was recorded. Flow rate was set at 300 µL/min for APCI interface. Ion source parameters used in APCI interfaces are listed in Table 5. In this table the collision gas value is only given in product ion scan mode and set at zero in Q1 scan mode.

Table 5 General ion source parameters in PI and NI modes for infusion MS experiments

	APCI	
	PI	NI
nebulizer current (µA)	5	-5
temperature (°C)	500	500
nebulizer gas (psi.)	32	32
auxiliary gas (psi.)	85	85
curtain gas (psi.)	60	60
collision gas (psi.)	1	1

4.2.2 LC/MS/MS analysis

The intermediates were separated on LiChrospher®60 RP-select B column using the time-scheduled ion detection program according to Table 6 and 7. The gradient elution steps for APCI interface were operated as shown in Table 8.

Table 6 Optimal parameters of purposed intermediates in product scan mode with time-scheduled detection program for LC/APCI/MS/MS, NI mode

Compound	MS/MS Transition	Compound parameters (Volts)					
		DP	FP	EP	CEP	CE	CXP
Maleic acid	115 → 71	-16	-270	4	-14	-10	-12
Anthranilic acid	136 → 92	-16	-340	10.5	-14	-20	-18
Benzoic acid	121 → 77	-11	-270	5.5	-14	-15	-14

Table 7 Optimal parameters of purposed intermediates in product scan mode with time-scheduled detection program for LC/APCI/MS/MS, PI mode

Compound	MS/MS Transition	Compound parameters (Volts)					
		DP	FP	EP	CEP	CE	CXP
Phthalic acid	167 → 149	61	370	12	2	15	11
	→ 121	61	370	-12	12	25	9
3-aminophenol	110 → 93	26	280	-10.5	20	20	5
	→ 65	26	280	-10.5	20	30	10
Toluidine	108 → 91	26	340	-11	18	25	6
	→ 65	26	340	-11	18	35	7
Benzidine	185 → 168	31	360	-11	12	25	15
	→ 151	31	360	-11	12	35	21
Tolidine	213 → 196	41	360	-11.5	14	25	20
	→ 181	41	360	-11.5	14	35	22
8-amino-1-naphthol-3,6-disulfonic acid disodium salt	319 → 151	26	350	-12	20	15	11
	→ 133	26	350	-12	20	20	17

Table 8 Gradient mobile phase for LC/APCI/MS/MS analysis

Time (min)	Flow rate (mL/min)	Methanol (%)	Water (%)
0	1.0	0	100
2.50	1.0	0	100
3.00	1.0	20	80
5.50	1.0	20	80
10.00	1.0	80	20
12.00	1.0	90	10
17.00	1.0	90	10
17.10	1.0	0	100

4.3 Ion chromatography

The concentrations of low molecular weight aliphatic acids such as formic, acetic, maleic acid etc., and inorganic anion including SO_4^{2-}, NO_3^-, NO_2^- etc., were determined using ion chromatography. Temperature oven at 30 °C and AS17 (250 mm x 2 mm) column 10 µL sample loop at a flow rate of 0.25 mL/min was studied. The optimized gradient profile is detailed in Table 9.

Table 9 Gradient profile for the chromatographic separation of anion intermediates by anion-exchange IC

Time (min)	Concentration of KOH (mM)	Curve	Comment
Initial	5.00	-	
0.00	5.00	5	
3.00	5.00	5	Sample injection
8.00	20.00	5	
10.00	10.00	5	
15.00	10.00	5	
30.00	30.00	1	End of step gradient
30.10	5.00	1	

5. Application of the method

5.1 Photodegradation of Trypan Blue under natural sun light

Ten milliliters of solution containing 2.08×10^{-5} M (corresponding to 20 mg/L) of Trypan Blue at pH 7 and 1.5 mg of photocatalyst (0.36 wt% Au loading and TiO_2 without gold loading) was used. The experiment was carried out as described in section 3.1. Then, the suspension solution was irradiated under the sun light. The Lux/FC light meter was used to measure the intensity of light. Absorbance change was monitored by UV/VIS spectrophotometer.

5.2 Photodegradation of wastewater

The wastewater sample used in this study was reactive dye group. The original wastewater characteristics are shown in Table 10. The wastewater sample was filtered through 110 mm Whatman No.42. The pH value was adjusted to 7 with dilute sodium hydroxide and acetic acid. Then the solutions were carried out as described in section 4. The degraded solutions were analyzed using UV/VIS spectrophotometer, LC/DAD spectrophotometer and Ion chromatography after five-fold dilution of the filtrate.

5.3 Photodegradation of Trypan Blue spiked in wastewater

The 5.20×10^{-5} M of Trypan Blue was prepared by dissolving 5 mg of Trypan Blue in wastewater adjusted to pH 7, then diluted to final volume of 100 mL with wastewater. The decrease in Trypan Blue was monitored by LC/DAD spectrophotometer.

Table 10 The physical properties of original wastewater

Type of Wastewater	Color	pH
Reactive Dye	Red	11

RESULTS AND DISCUSSION

1. Absorption characteristics of dye

The absorption spectrum of aqueous Trypan Blue is shown in Figure 4. It absorbs strongly in the visible region with maximum absorption located at 596 nm (chromophore-containing azo linkage). Other three bands are in the ultraviolet region including at 215 nm (benzene and naphthalene rings), 237 nm (benzene rings) and 316 nm (naphthalene rings). The assignments of the peaks based on the Stylidi *et al.*, 2003. The molar absorption coefficients are ε_{237} = 35,688, ε_{316} = 19,481 and ε_{597} = 51,408 M^{-1} cm^{-1}, respectively, base on the given molecular weight of Trypan Blue.

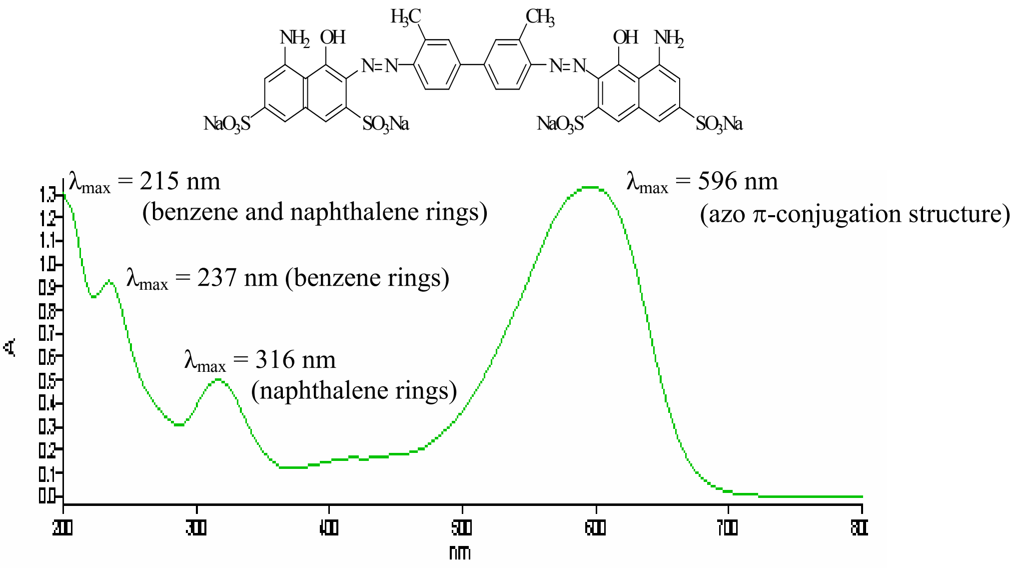

Figure 4 Absorption spectrum of the aqueous solution of 2.60 x 10^{-5} M Trypan Blue at pH 7

2. Characterization of gold/TiO$_2$

Scanning electron micrograph of 0.36% Au/TiO$_2$ particles is shown in Figure 5. The gold particles appear to be very nearly spherical. The yields of gold doped on TiO$_2$ and gold residue in filtrate are listed in Table 11. As shown in Table 11, the percentage of Au deposition on TiO$_2$ is not 100 % in every case. The found values were quoted for wt% Au in the subsequent studies.

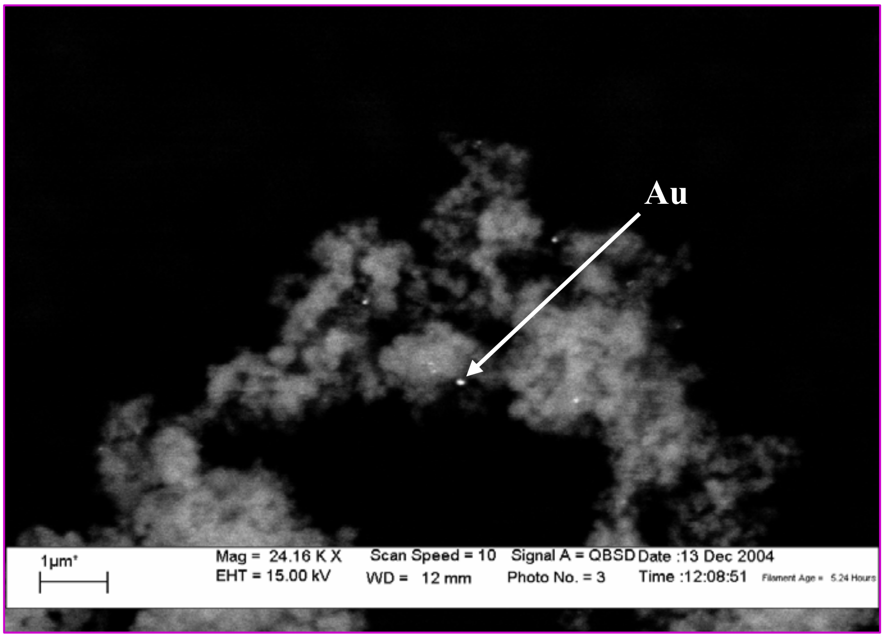

Figure 5 Scanning electron microscope (SEM) image of 0.36 wt% Au/TiO_2 particles calcined at 400 °C

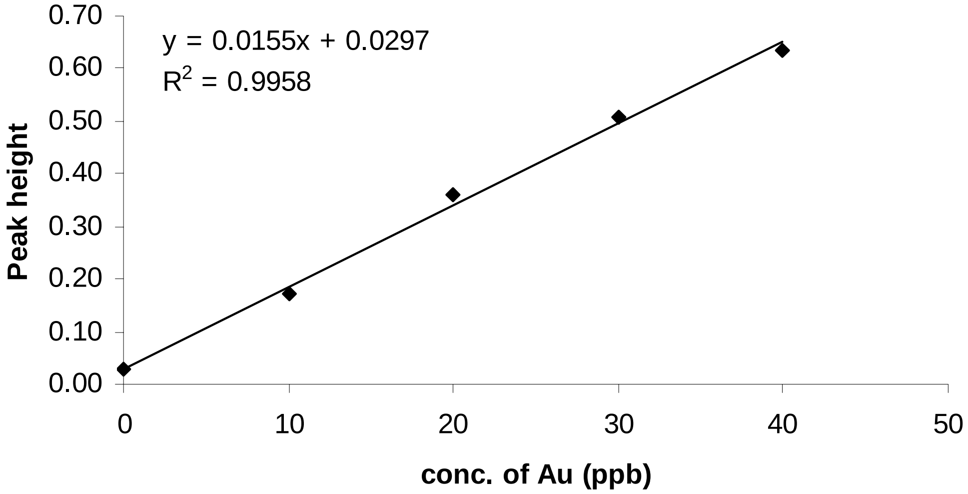

Figure 6 Calibration curve of the determination of gold by graphite furnace AA spectrometer, instrumental parameters as described in Table 2

Table 11 The yield of gold on TiO_2 in the term of wt% using graphite furnace AA spectrometer

Loading of Au on TiO_2 (%wt) ± SD	Color	Percentage of Au deposition (%)	Percentage of Au in residue (%)
0.0714 ± 0.0187	Fade pink-purple	71.40	0.10
0.3615 ± 0.0196	Pink-purple	72.30	1.76
0.8030 ± 0.0040	Purple	80.30	1.98
1.3581 ± 0.0912	↓	90.54	not detected
1.8867 ± 0.0597	Dark purple	94.34	not detected

3. Photocatalysis degradation of Trypan Blue

The mechanism of the photocatalytic oxidation process using TiO_2 is briefly explained as follows: conduction band electrons (e_{CB}^-) and valence band (h_{VB}^+) are generated when aqueous TiO_2 suspension is irradiated with light energy equal or greater than its band gap energy (3.2 eV), equivalent to about 400 nm. Therefore TiO_2 is only photoexcited by near-UV illumination (300 – 400 nm) following the reaction in equation (1). The photogenerated electrons can directly reduce the dye or react with electron acceptors such as O_2 adsorbed on the Ti(III)-surface or dissolved in water to superoxide radical anion ($O_2^{\bullet-}$). Besides, the photogenerated holes can oxidize the organic molecule to form R^+ or react with OH^- and H_2O oxidizing them into $^{\bullet}OH$. Other highly oxidant species such as peroxide radicals are reported also to be responsible for the heterogeneous. The relevant reactions at the semiconductor surface causing the degradation of dyes can be summarized as follows:

$$TiO_2 \quad + \quad h\nu \quad \rightarrow \quad TiO_2\,(e^-_{CB}, h^+_{VB}) \qquad (1)$$

The valence band holes (h^+) migrate to the interface and react with OH^- or H_2O adsorbed onto the TiO_2 to create hydroxyl radicals ($^{\bullet}OH$).

$$TiO_2(h_{VB}^+) \ + \ OH^- \ \rightarrow \ TiO_2 + OH^{\bullet} \qquad (2)$$
$$TiO_2(h_{VB}^+) \ + \ H_2O \ \rightarrow \ TiO_2 + H^+ + OH^{\bullet} \qquad (3)$$

In the conduction band, the photoinduced electrons (e^-) react with electron acceptors such as O_2 to form a superoxide ions ($O_2^{\bullet-}$) which combine with protons to create peroxyl radical ($HO_2^{\bullet}$), particularly in acid media.

$$TiO_2(e_{CB}^{-}) + O_2 \rightarrow TiO_2 + O_2^{\bullet -} \quad (4)$$
$$O_2^{\bullet -} + H^+ \rightarrow HO_2^{\bullet} \quad (5)$$
$$\text{Dye} + {}^{\bullet}OH \rightarrow \text{degradation products} \quad (6)$$
$$\text{Dye} + h_{VB}^{+} \rightarrow \text{oxidation products} \quad (7)$$
$$\text{Dye} + e_{CB}^{-} \rightarrow \text{reduction products} \quad (8)$$
$$e^- + h^+ \text{ pairs} \rightarrow \text{recombination} \quad (9)$$

$$\text{Dye} + {}^{\bullet}OH, O_2^{\bullet -} \text{ or } HO_2^{\bullet} \rightarrow SO_4^{2-}, NO_3^{-}, NH_4^{+}, CO_2 \text{ and } H_2O \quad (10)$$

These radicals (${}^{\bullet}OH$, $O_2^{\bullet -}$ and $HO_2^{\bullet}$) are very strong oxidizing and they are able to decompose the dyes to the oxidation products. Eventually, the parent compounds and their intermediates will be oxidized into inorganic products (SO_4^{2-}, NO_3^{-}, NH_4^{+}), CO_2 and water (Bandara *et al.*, 1999, Tanaka *et al.,* 2000, Galindo *et al.,* 2000 and Daneshva *et al.,* 2003).

In the case of gold/TiO_2, the formation of e^- and h^+ as follow (Dawson and Kamat, 2001):

$$(TiO_2)Au + h\nu \rightarrow (TiO_2(e^- + h^+))Au \quad (11)$$

Au doping leads to appearance of a new electronic state and the change of band gap energy ($E_g < 3.2$ eV). Hence, the excitation energy is expanded from UV light of TiO_2 to visible light of Au/TiO_2. When TiO_2 particles are doped with Au particles, the photogenerated electrons can transfer from TiO_2 to Au and then be stored, which facilitates the separation of the photogenerated electron and hole, that is decreasing electron-hole pairs recombination. In this case, the efficiency of photocatalysis is improved (Wang *et al.,* 1998).

Trypan Blue was chosen as a model of pollutant due to its toxicity and chemical resistance to degradation. When the suspension was irradiated with the solar light-simulating source, relatively rapid decolorisation of the solution took place. The complete decolorisation of dye was observed after 40 h of irradiation. As shown in Figure 7, the color of Trypan Blue changed from blue to purple, brown, yellow and colorless, respectively. The color of organic colorant reduces when the cleavage of -N=N- bonds, the -C=C- bonds, heterocyclic and aromatic rings occur. The absorption band at 596 nm rapidly decreases as shown in Figure 8 suggests that the chromophore responsible for the characteristic color of the azo dye is destroyed. The characteristic absorption peak of Trypan Blue at $\lambda = 596$ nm disappeared completely after 25 h of photocatalysis, indicating that the azo -N=N- conjugate structure is completely destroyed. Maximum absorption wavelength in the visible range shifts to the shorter wavelength (Hypsochromic shift) with an increase in irradiation time. In addition, the pH of the solution during degradation gradually decreases from 7 to 4 after irradiation for 70 h.

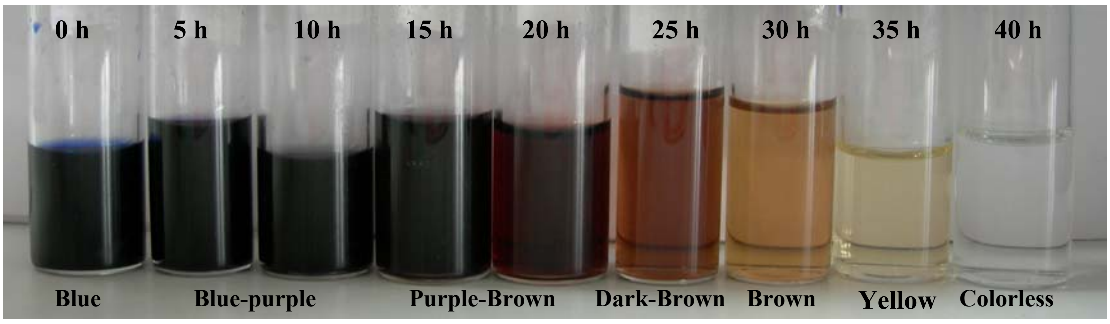

Figure 7 Color change of 2.60 x 10^{-4} M Trypan Blue at pH 7 (natural) with 5 gL^{-1} of 0.36 wt% gold/TiO_2 suspension following photocatalytic degradation at various irradiation time

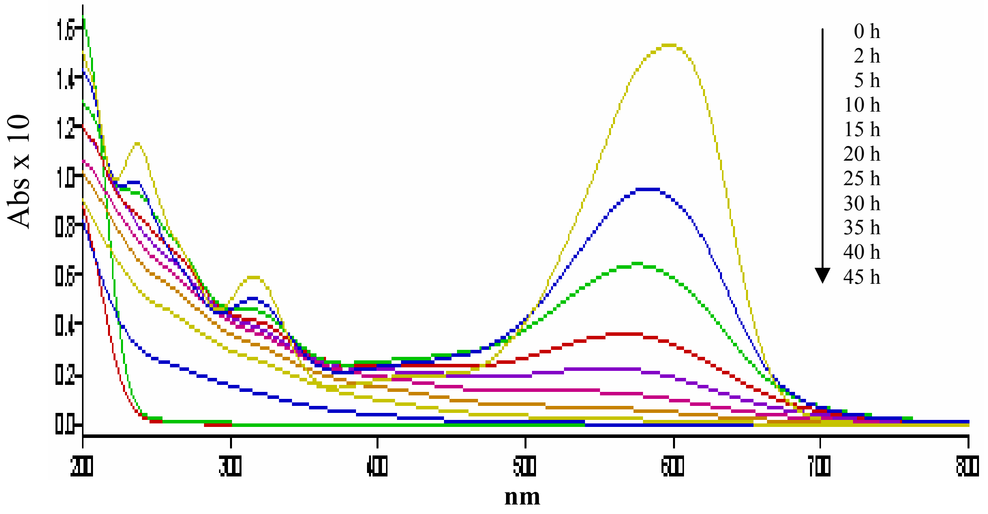

Figure 8 Absorption spectra of 2.60 x 10^{-4} M Trypan Blue at pH 7 (natural) with 5 gL^{-1} of 0.36 wt% gold/TiO_2 suspension following photocatalytic degradation at various irradiation time

The efficiency of photocatalytic degradation was calculated for each experiment as function of kinetic constant. When the first order kinetics sufficiently characterized the reaction rate, it could be expressed as:

$$R = \frac{-d[\mathrm{C}]}{dt} = k[\mathrm{C}] \qquad (12)$$

When k is first order rate constant (min^{-1}), R is reaction rate (Mol L^{-1} min^{-1}) and C is initial concentration (Mol L^{-1}) of the reactant. Integration of equation 12 is:

$$\ln \frac{C_t}{C_0} = -kt \qquad (13)$$

When C_0 and C_t are concentration at the beginning and at a certain time (Mol/L), t is the irradiation time (min). According to the relationship between the concentration and absorption of the solution, it was also expressed as:

$$\ln \frac{A_t}{A_0} = -kt \qquad (14)$$

Hence, a plot of $\ln(A_t/A_0)$ versus irradiation time should give a straight line whose slope equals the first order rate constant, k. For half-life of first order kinetics will be corresponding with the first order rate constant, it was also expressed as:

$$t_{1/2} = \frac{0.693}{k} \qquad (15)$$

When $t_{1/2}$ is half-life of first order kinetics (min)

3.1 Effect of gold loading on TiO_2 on photodegradation of Trypan Blue

Gold doped TiO_2 was prepared by adsorption of $[AuCl_4]^-$ ions on TiO_2 surface followed by reduction with $NaBH_4$. After the dropwise addition of $NaBH_4$, colloidal gold/TiO_2 suspension changes to pink-purple in the gold loading of 0.07 and 0.36 wt% on TiO_2 and to purple in the case of 0.80, 1.36 and 1.89 wt%. It should be noted that the dark purple at the higher concentration of gold more than at the low concentration. To evaluate the photodegradation activity of the prepared catalysts compared with bare TiO_2 and to determine an optimum dosage of gold doped on TiO_2, the photocatalytic degradation of aqueous solution of Trypan Blue is carried out. As shown in Figure 9, it is indicated that the efficiency of Trypan Blue decolorisation using the TiO_2 powder doped with gold is significantly higher than that of using the pure TiO_2 powder. Besides, the photocatalytic efficiencies are enhanced with an increase in the gold loading. The rate of photodegradation is almost constant when wt% Au is in the range 0.36–1.36 %. However, further increase of gold loading on TiO_2 to 1.89 wt% decreases photocatalytic efficiency due to the excess loading of metal particles may cover active sites on the TiO_2 surface, thereby decreasing photodegradation efficiency (Sakthivel *et al.,* 2004). Therefore, a significant decrease of the photocatalytic efficiency is observed at higher gold loading.

Figure 10 shows the initial first order kinetics of photodegradation, only first 30 min of irradiation are calculated. Their rate constants are also presented in Figure 11 and listed in Table 12. Therefore, 0.36 wt% gold was chosen for further studies.

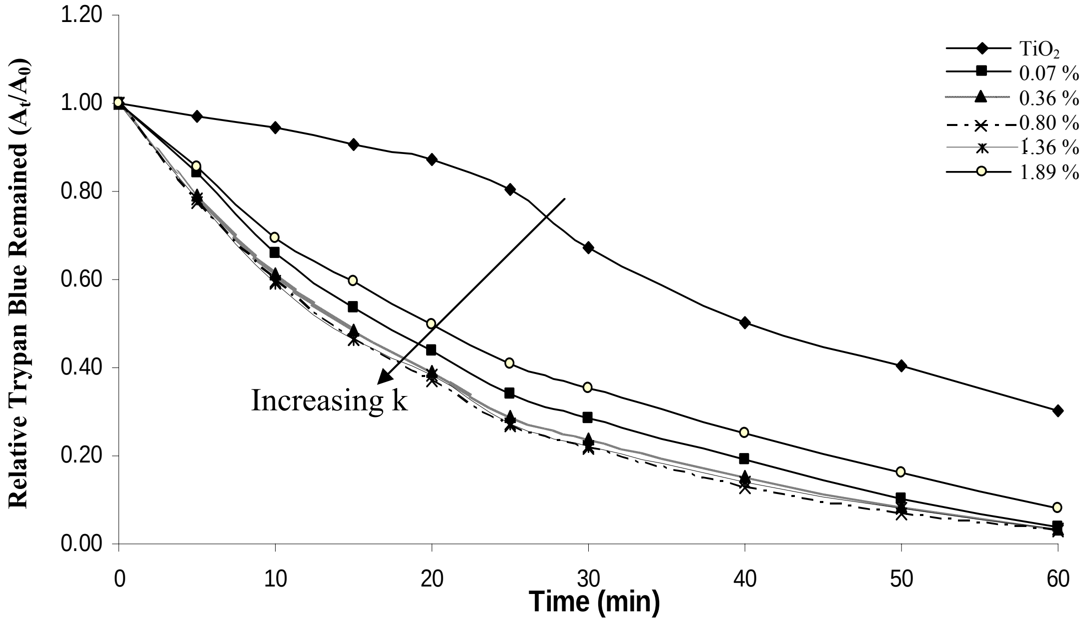

Figure 9 The exponential decay of Trypan Blue in a first order reaction of 5.20×10^{-5} M, pH 7

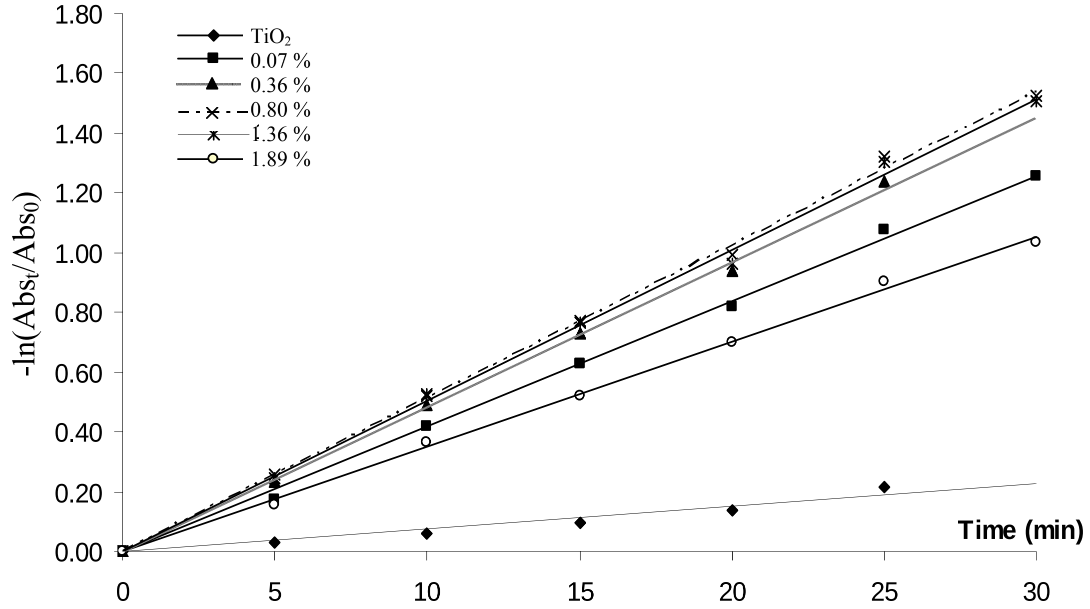

Figure 10 The first order kinetics of Trypan Blue photodegradation in the presence of gold/TiO_2 with an initial concentration of 5.20×10^{-5} M, pH 7

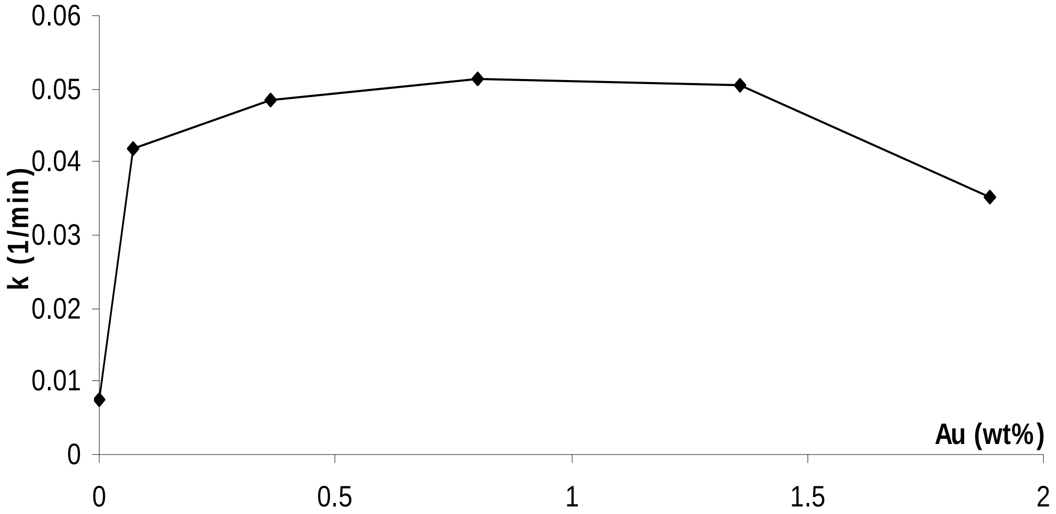

Figure 11 The first-order rate constants (k) of Trypan Blue photodegradation in the presence of gold/TiO_2 in term of wt% with an initial concentration of 5.20 x 10^{-5} M, pH 7

Table 12 Apparent first-order rate constant (k), reaction rate (R) and $t_{1/2}$ of the photodegradation of 5.20 x 10^{-5} M Trypan Blue at different gold loading

Au (wt%) on TiO_2	Kinetic constant, k (min^{-1})	Correlation coefficient, R^2	Reaction rate, R x 10^6 (Mol $L^{-1}min^{-1}$)	Half-life, $t_{1/2}$ (min)
0	0.0075	0.9482	0.390	92.4000
0.0714	0.0419	0.9980	2.179	16.5394
0.3615	0.0485	0.9986	2.522	14.2887
0.8030	0.0513	0.9985	2.668	13.5088
1.3581	0.0505	0.9976	2.621	13.7228
1.8867	0.0351	0.9984	1.825	19.7436

The observed enhancement in the presence of gold on TiO_2 is attributed to the acceleration of hydroxyl radical formation. In addition, the presence of gold on TiO_2 favors the migration of produced electrons to gold, thus improving the electron-hole separation, that is, decreasing electron-hole pairs recombination, consequently, the photocatalytic efficiency increases. However, it should be emphasized that the heterogeneous photocatalysis is a surface process and the gold-supported catalysts have different surface characteristics. This results in differences in the total titania surface area exposed to the light beam and that available for pollutant adsorption (Bamwenda *et al.,* 1995, Li 2002, Arabatzis *et al.*, 2003 and Sakthivel *et al.*, 2004).

3.2 Effect of calcination temperature on photodegradation of Trypan Blue

Dried gold/TiO_2 catalysts are gray-purple. After calcination, the color is still gray-purple at 200 °C, changes to gray at 300 °C and to purple after calcination at temperatures above 400 °C. For high calcination temperatures at 400, 500 and 600 °C, purple color of the catalysts gradually change to dark purple when calcination temperature increases. Purple color is the characteristic of metallic gold particles (Zanella *et al.,* 2004 and Bamwenda *et al.,* 1995).

The catalysts obtained at various temperatures for calcination were tested in photodegradation reaction of 5.20 x 10^{-5} M Trypan Blue with an initial pH of 7 as a function of irradiation time under simulating solar light. Figure 12 shows relative decay of dye. It is found that the photocatalytic efficiency increases with increasing in the calcination temperature up to 400 °C. At the calcination temperature of 400, 500 and 600 °C, their photocatalytic efficiencies are almost the same. First order kinetics of photodegradation are presented in Figure 13 and their rate constants are also compared in Figure 14 and Table 13.

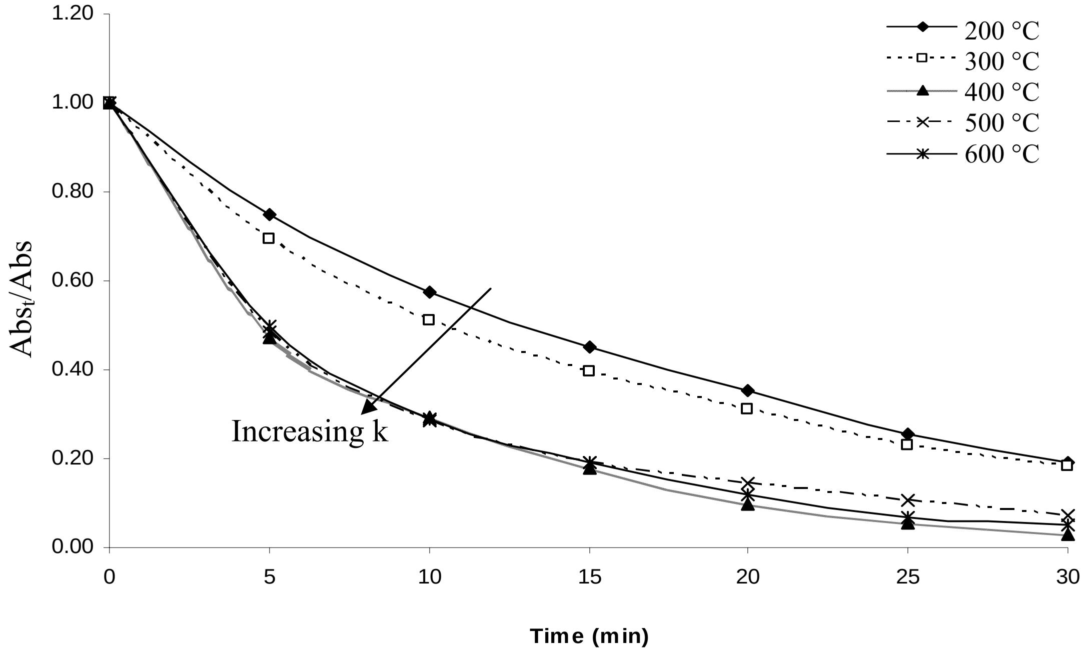

Figure 12 The exponential decay of the reactant in a first-order reaction of 2.60 x 10^{-5} M of Trypan Blue (corresponding to 25 mg/L), an initial pH 7, in the presence of 0.36 wt% gold/TiO_2 at various calcination temperatures

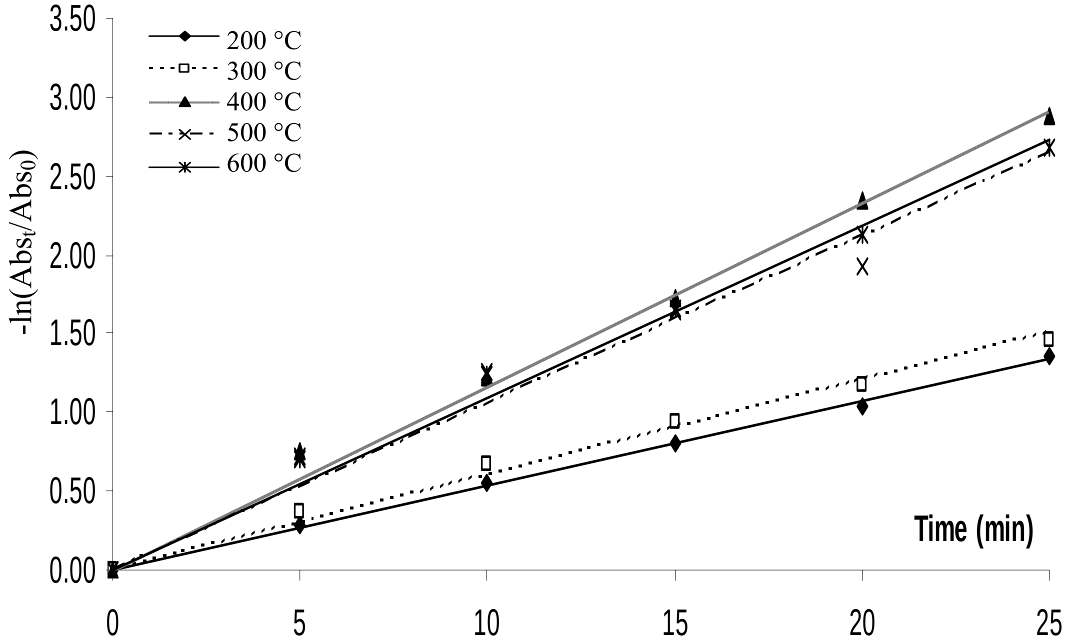

Figure13 The first order kinetics of Trypan Blue photodegradation in the presence of 0.36 wt% gold/TiO_2 with an initial concentration of 2.60 x 10^{-5} M, pH 7

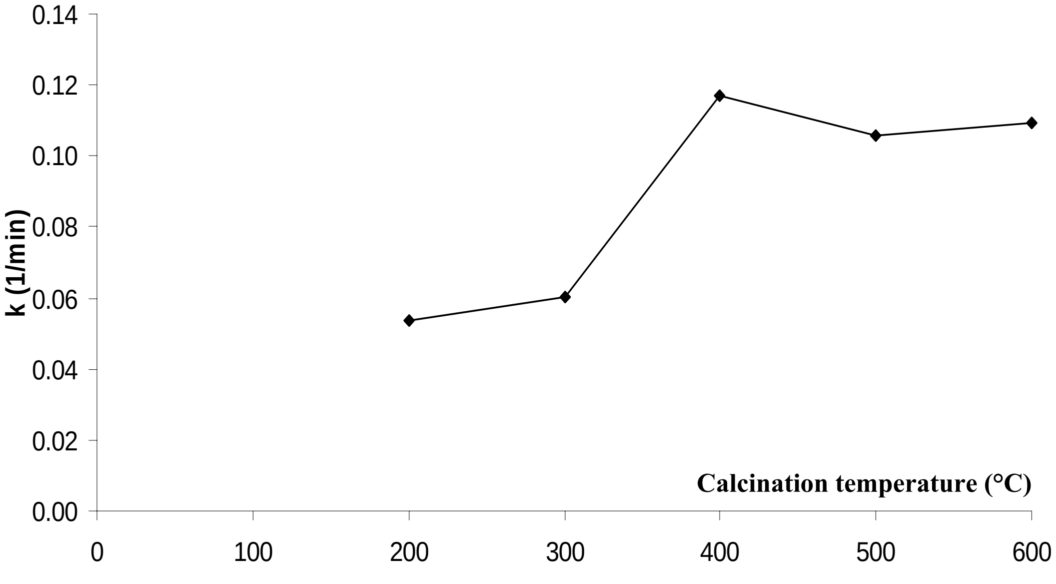

Figure14 The first-order rate constants (k) of Trypan Blue photodegradation in the presence of 0.36 wt% gold/TiO_2 with an initial concentration of 2.60 x 10^{-5} M, pH 7

Table 13 Apparent first-order rate constant (k), reaction rate (R) and $t_{1/2}$ of the photodegradation of 2.60 x 10^{-5} M Trypan Blue at various calcination temperatures

Calcination Temp.(°C)	Kinetic constant, k (min^{-1})	Correlation coefficient, R^2	Reaction rate, R x 10^6 (Mol $L^{-1}\text{min}^{-1}$)	Half-life, $t_{1/2}$ (min)
200	0.0536	0.9978	1.3936	12.9291
300	0.0601	0.9912	1.5626	11.5308
400	0.1168	0.9939	3.0368	5.9332
500	0.1057	0.9516	2.7482	6.5563
600	0.1093	0.9886	2.8418	6.3403

3.3 Effect of initial pH of an aqueous Trypan Blue on photodegradation of Trypan Blue

The degradation of Trypan Blue at 2.08 x 10^{-5} M (corresponding to 20 mg/L) was studied at different initial pH levels ranging from 3 to 11. The pH of dye affects not only the surface properties of TiO_2 but also the dissociation of Trypan Blue. The properties of TiO_2 surface at acidic and alkaline media are shown in equation (16) and (17), respectively (Konstantinou and Albanis, 2004).

$$TiOH + H^+ \leftrightarrow TiOH_2^+ \quad \text{(acidic media)} \quad (16)$$
$$TiOH + OH^- \leftrightarrow TiO^- + H_2O \quad \text{(alkaline media)} \quad (17)$$

Thus, the TiO_2 surface is positively charged in acidic media, whereas it is negatively charged under alkaline media. Trypan Blue is totally dissociated in aqueous media. In acidic media, Trypan Blue is in the acid form which dissociated less than in the basic form. Thus, at low pH, the undissociated acidic Trypan Blue is adsorbed onto the positive TiO_2 surface. At high pH, adsorption is reduced because either the dissociated Trypan Blue (sulfonate anion), or the TiO_2 surface becomes negatively charged (Reutergårdh and Iangphasuk, 1997 and Poulios and Tsachpinis, 1999).

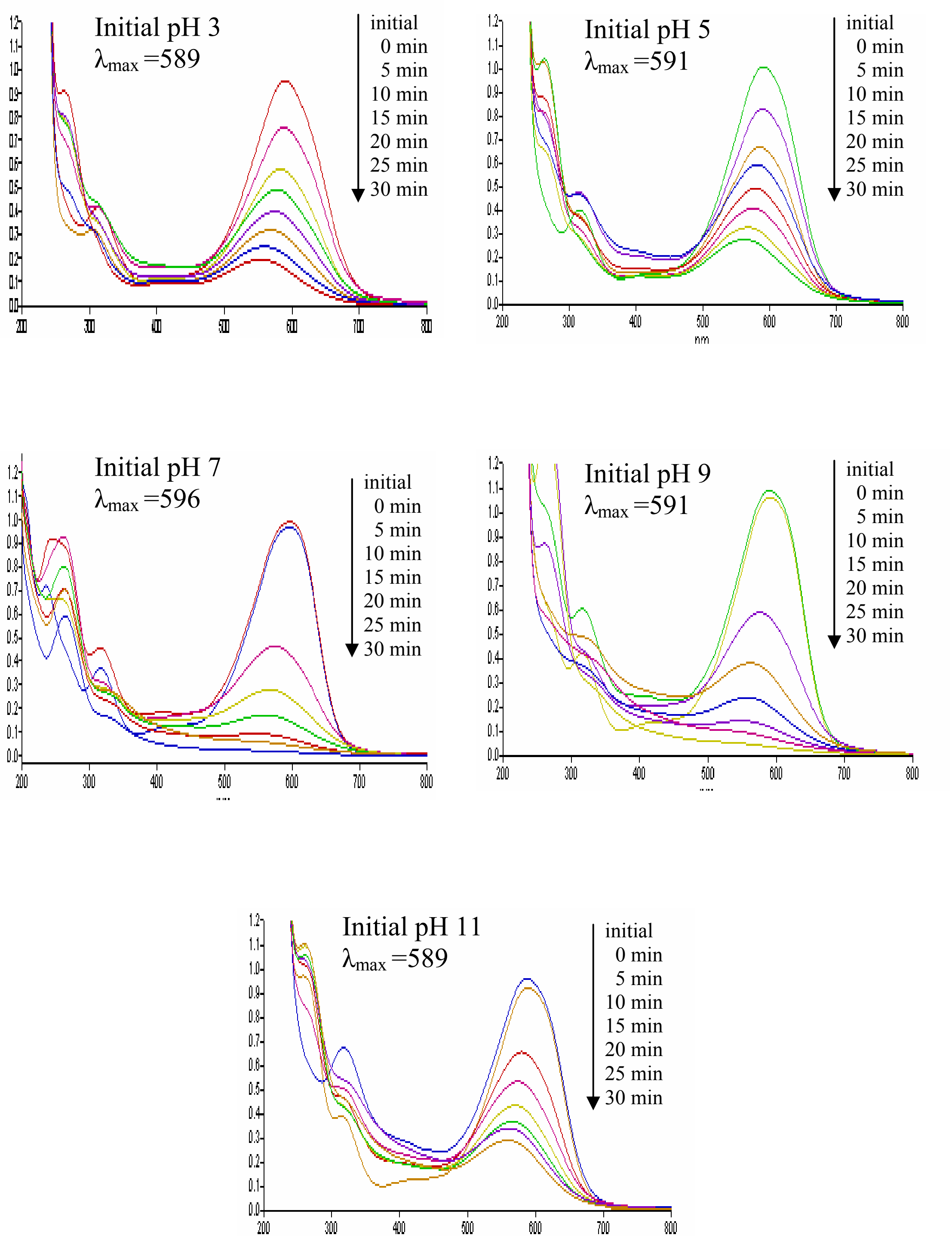

Figure15 UV/VIS spectral change of Trypan Blue in the presence of gold/TiO_2 as a function of irradiation time (initial represents to absorption spectrum before the addition of the photocatalyst). Experimental conditions: [Trypan Blue] = 2.08×10^{-5} M, 8 mL, [gold/TiO_2] = 2.5 mg

The effect of pH on mechanisms of photocatalytic degradation is rather complicated. Generally, three mechanisms, namely hydroxyl attack, positive hole oxidation and reduction by electron in conduction band, may contribute to the degradation of dye depending upon the nature of substrate and the solution pH (Tang *et al.,* 1997). Hydroxyl radicals are formed by the reaction between hydroxide ions and positive holes. The positive holes are considered as the major oxidation species at neutral or high pH levels. It was stated that in alkaline solution, $^{\bullet}OH$ are easier to be generated by oxidizing more hydroxide ions available on TiO_2 surface, thus the efficiency of the process is enhanced. However, it should be noted that in alkaline solution there is a Culombic repulsion between the negative charged surface of photocatalyst and the hydroxide anions. This fact could prevent the formation of $^{\bullet}OH$ and thus decreasse the photooxidation. At low pH, reduction by electrons in conduction band may play a very important role in the degradation of dyes due to the reductive cleavage of azo bonds.

Figure 15 demonstrates the UV/VIS spectral change of Trypan Blue as a function of irradiation time at various pH. At the acidic media, pH 3 and 5, the spectrum looks similar to each other, but they are different from the absorption of aqueous Trypan Blue at neutral and alkaline media. It, also, should be noted that the absorption intensities decrease without illumination at the pH 3 and 5. This may be due to the effect of the electrostatic attraction of the positively charged TiO_2 with sulfonic groups of dissociated Trypan Blue, and adsorption of undissociated Trypan Blue. This result is confirmed with the color change of used catalysts. Pink-purple catalysts change to blue after using in acidic media but they are still pink-purple in neutral and alkaline media. On the other hands, there is no absorption intensity change after adding catalysts and stirring in dark condition at the pH of 7, 9 and 11. After irradiation, the absorption intensities rapidly decrease at both neutral and alkaline media.

The first-order kinetics of Trypan Blue photodegradation are described in Figure 16 and the observed rate constants are shown in Figure 17. The first order rate constants of photooxidation of Trypan Blue in the neutral and alkaline media are clearly higher than in acidic media. The k values for degradation, also, are listed in Table 14 along with the value of $t_{1/2}$ at different initial pH of solution. As mentioned before, sulfonic groups in Trypan Blue strongly adsorb on TiO_2 at low pH. This behavior decreases the active centers on the catalyst surface. The observed photooxidation rate is highest at pH 7 and decreases with the increase in the initial pH. This may be due to the excess of OH^- on the catalyst surface, which favors the photogeneration of $^{\bullet}OH$. In alkaline solution, there is a Culombic repulsion between the negative charged surface of photocatalyst and the hydroxide anions. This fact could prevent the formation of $^{\bullet}OH$ and thus decreases the photooxidation. Therefore, an optimum pH of Trypan Blue solution is 7and used for subsequent studies.

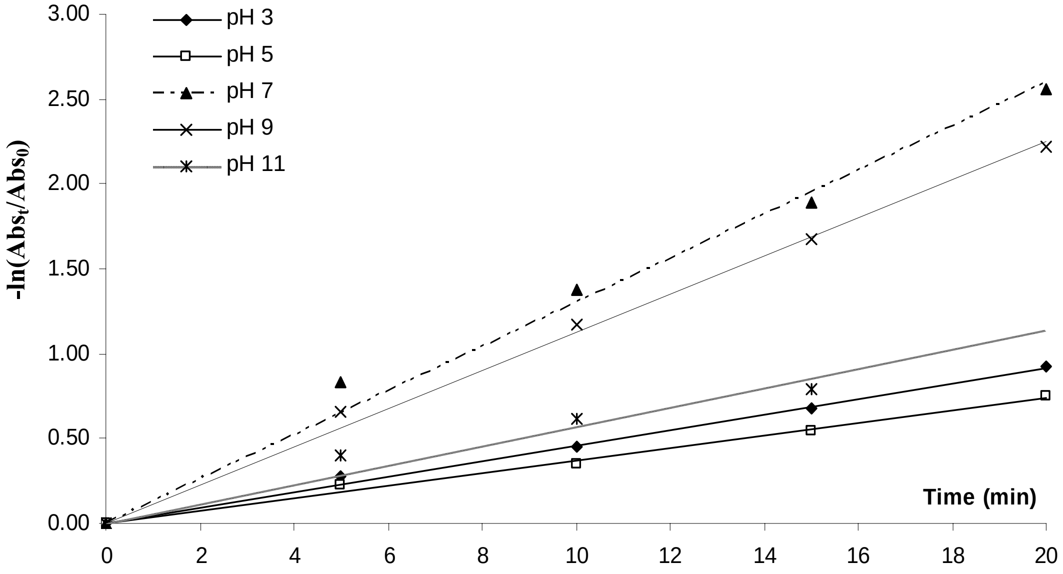

Figure16 The first order kinetics of Trypan Blue photodegradation in the presence of 0.36 wt% gold/TiO_2 at pH 7, 9, 11, 3 and 5, respectively

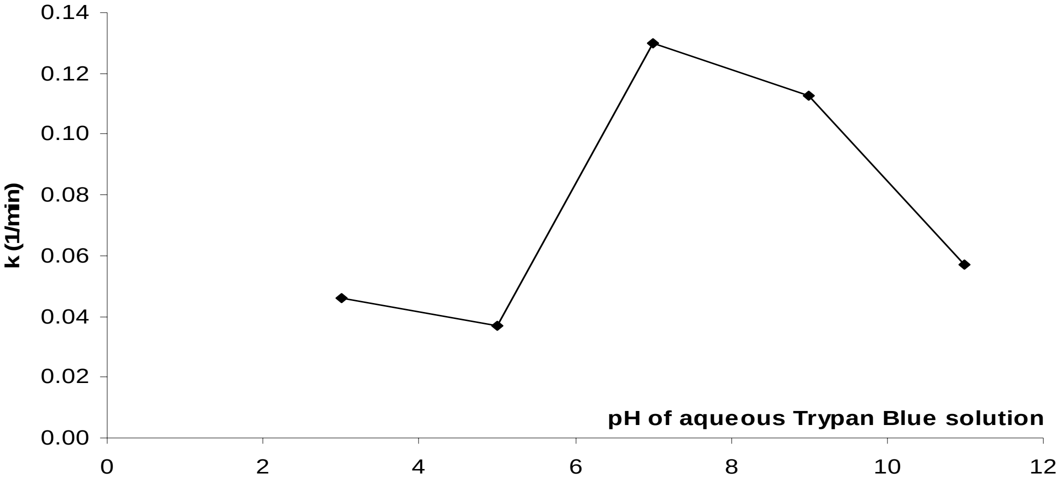

Figure17 The first-order rate constant (k) of Trypan Blue photodegradation in the presence of 0.36 wt% gold/TiO_2 with an initial concentration of 2.08 x 10^{-5} M

Table 14 Apparent first-order rate constant (k), reaction rate (R) and $t_{1/2}$ of the photodegradation of 2.08 x 10^{-5}M Trypan Blue at different pH levels

Dosage of gold/TiO_2 (gL^{-1})	Kinetic constant, k (min^{-1})	Correlation coefficient, R^2	Reaction rate, R x 10^6 (Mol $L^{-1}min^{-1}$)	Half-life, $t_{1/2}$ (min)
3.0	0.0459	0.9957	0.9547	15.0980
5.0	0.0371	0.9942	0.7717	18.6792
7.0	0.1301	0.9889	2.7061	5.3267
9.0	0.1126	0.9961	2.3421	6.1545
11.0	0.0570	0.9446	1.1856	12.1579

3.4. Effect of dosage of gold/TiO_2 on photodegradation of Trypan Blue

The experiments were carried out to assess the optimum catalyst loading by varying the amount of catalyst from 0.2 to 1.25 gL^{-1}. Figure 18 shows absorption spectra of 50 ppm Trypan Blue, pH 7 (natural) at various irradiation time. As the gold/TiO_2 dosage increase, the disappearance of Trypan Blue increases up to 1 gL^{-1}. Further increase in photocatalysts dosage only slightly enhance the efficiency of photodegradation of dye. Moreover, the disappearance hardly differs among 0.8, 1.0 and 1.25 gL^{-1} after illumination for 30 min. The first-order kinetics of Trypan Blue photodegradation are presented in Figure 19. The corresponding first order rate constants are shown in Figure 20 and listed in Table 15.

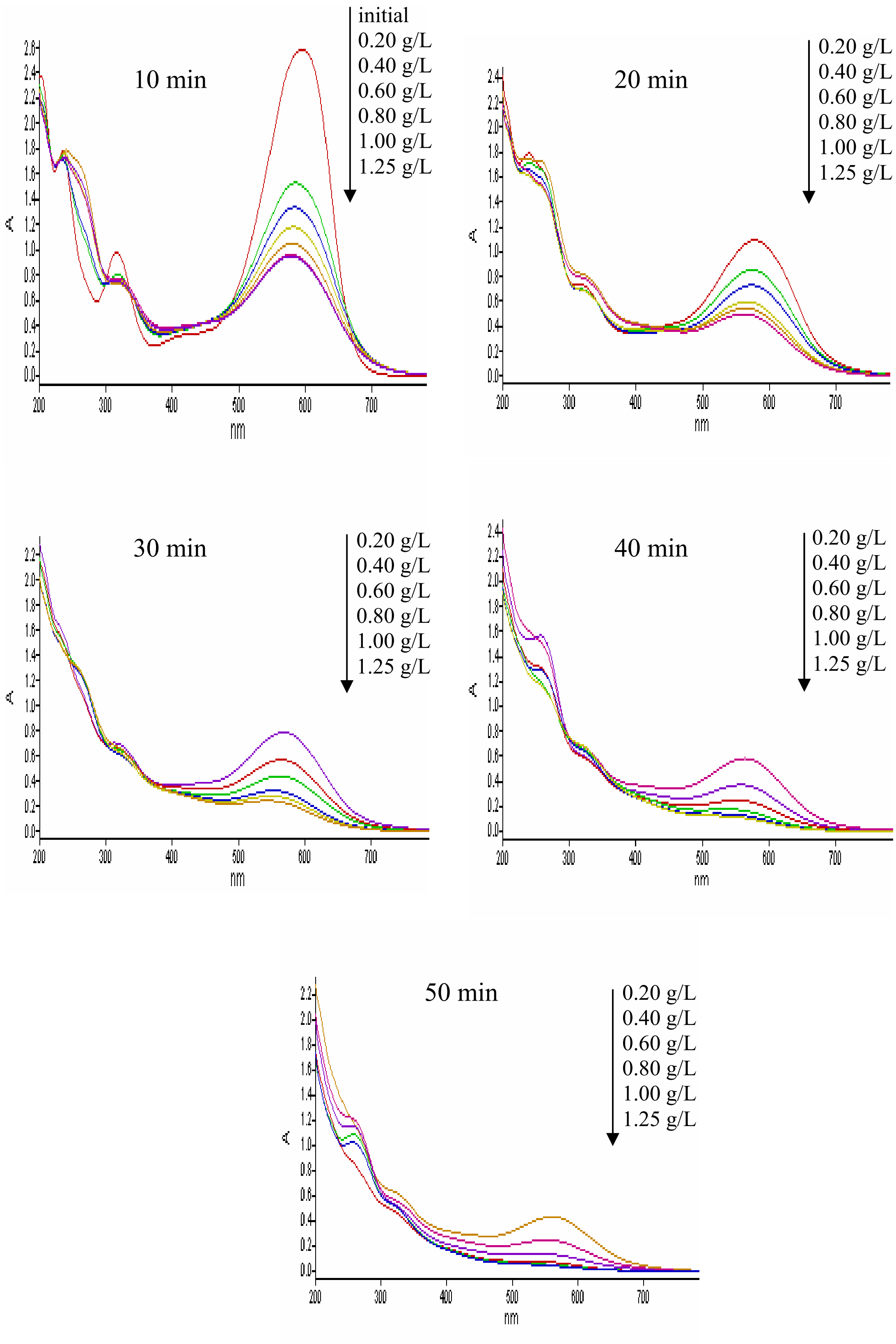

Figure 18 UV/VIS spectra of Trypan Blue in the presence of gold/TiO_2 as a function of irradiation time (initial represents to absorption spectrum before the addition of the photocatalysts). Experimental conditions, [Trypan Blue]= 5.20×10^{-5} M, 8 mL, pH 7

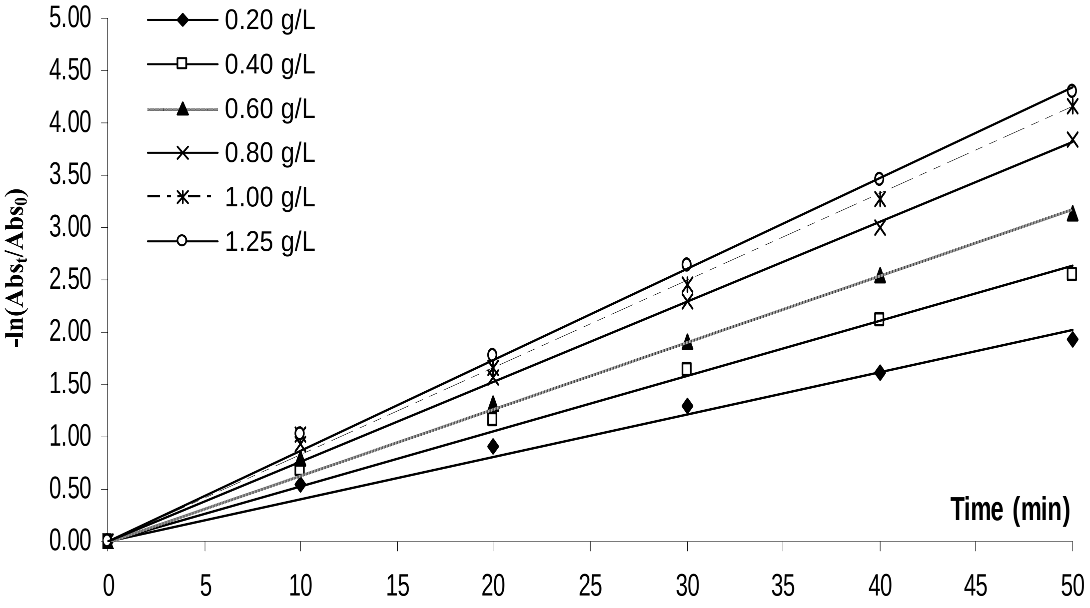

Figure 19 Relative absorbance vs. time profile during irradiation of Trypan Blue in an aqueous solution on the gold/TiO_2

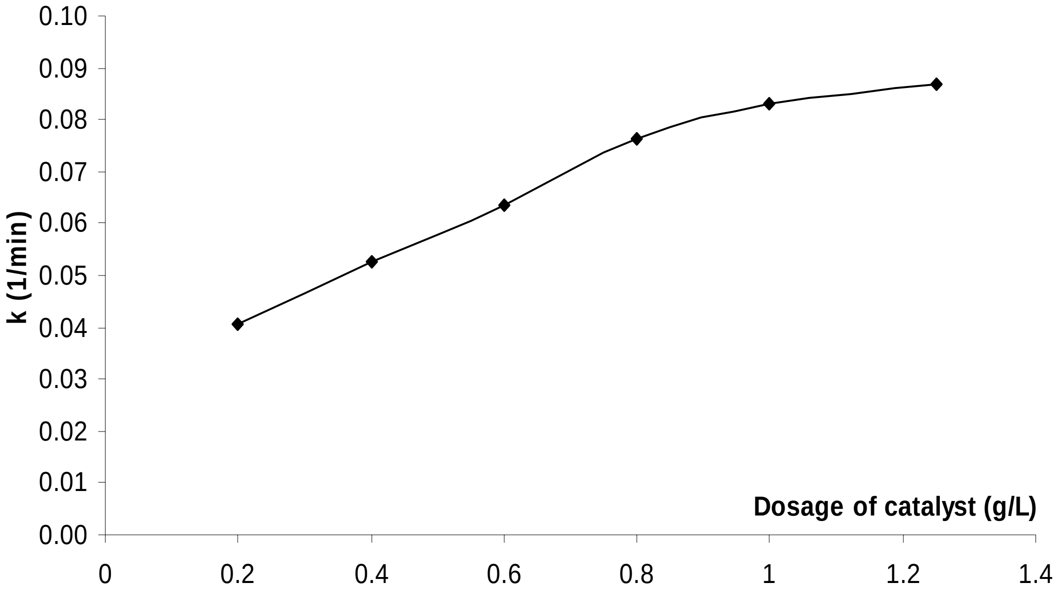

Figure 20 The first-order rate constants (k) of Trypan Blue photodegradation in the presence of 0.36 wt% gold/TiO_2 with an initial concentration of 5.20 x 10^{-5} M

Table 15 Apparent first-order rate constant (k), reaction rate (R) and $t_{1/2}$ of the photodegradation of 5.20 x 10^{-5} M Trypan Blue at different gold/TiO_2 dosages

Dosage of gold/TiO_2 (gL^{-1})	Kinetic constant, k (min^{-1})	Correlation coefficient, R^2	Reaction rate, R x 10^6 (Mol $L^{-1}min^{-1}$)	Half-life, $t_{1/2}$ (min)
0.20	0.0407	0.9854	2.1164	17.0270
0.40	0.0528	0.9894	2.7456	13.1250
0.60	0.0637	0.9952	3.3124	10.8791
0.80	0.0765	0.9969	3.9780	9.0588
1.00	0.0830	0.9966	4.3160	8.3494
1.25	0.0868	0.9975	4.5136	7.9839

The availability of active sites increases with the suspension of catalyst loading, but above the certain level of wt% Au leads to enhancement of the light reflectance and consequently decreases in the reaction rate. Hence, the amount of gold/TiO_2 was used at 1.0 gL^{-1} for the study of photocatalytic degradation. The optimum amount of gold/TiO_2 catalyst should be added in order to avoid unnecessary excess and also ensure total absorption of photons for efficient photomineralization. However, this optimum loading of photocatalyst is found to be dependent on the initial dye concentration (Konstantinou and Albanis, 2004).

3.5 Effect of concentration of Trypan Blue on photodegradation of Trypan Blue

The effect of initial concentrations of dye on the photodegradation efficiency as shown in Figure 20 was studied by varying the initial dye concentration; 2.08 x 10^{-5}, 2.60 x 10^{-5} and 5.20 x 10^{-5} M (corresponding to 20, 25 and 50 mg/L, respectively). The photodegradation of Trypan Blue is first-order kinetic reaction, also, shows in Figure 21 and the observed rate constants (k) are listed in Table 16 along with the value of $t_{1/2}$. Generally, the photodegradation rate decreases with the increase in initial dye concentration. Obviously, the generated radicals at high dye concentration are reduced since the active sites are covered by dye ions. Furthermore, a significant amount photons which generated from light source, may be adsorbed by the dye molecules rather than the TiO_2 particles. Consequently, $^{\bullet}OH$ and $O_2^{\bullet-}$ decrease and that reduce the efficiency of the photocatalysts. At higher dye concentration, thus, the requirement of catalyst surface needed for the degradation also increases.

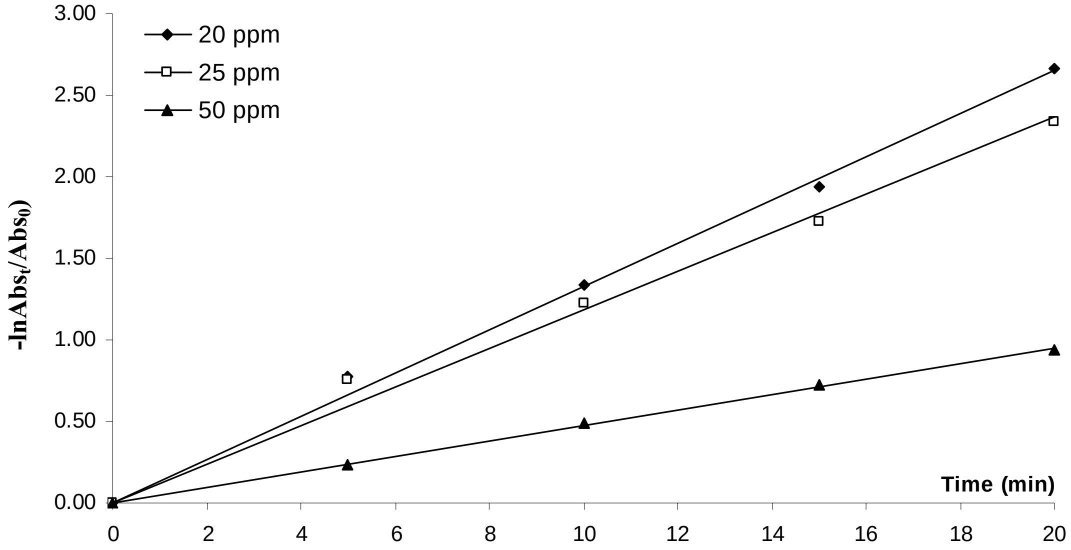

Figure 21 Degradation of various initial concentrations of Trypan Blue with 0.36 wt% gold/TiO_2 and initial pH 7

Table 16 Apparent first-order rate constant (k), reaction rate (R) and $t_{1/2}$ of the photodegradation of various initial concentrations of Trypan Blue with 0.36 wt% gold/TiO_2 and initial pH 7

Concentration of Dye (mg L^{-1})	Kinetic constant, k (min^{-1})	Correlation coefficient, R^2	Reaction rate, R x 10^6 (Mol $L^{-1}min^{-1}$)	Half-life, $t_{1/2}$ (min)
20	0.1328	0.9962	2.7622	5.2184
25	0.1183	0.9906	3.0758	5.8580
50	0.0476	0.9991	2.4752	14.5588

4. Kinetic and intermediate analysis

4.1 Kinetic study of Trypan Blue

Focusing on kinetic and intermediate analysis, the experiment was carried out under optimum conditions by adding 1.0 g/L of 0.36 wt% gold/TiO_2 (calcination temperature = 400°C) into 100 mL of 5.20 x 10^{-5} M (corresponding to 50 mg/L) of Trypan Blue, and pH value of 7 (Natural). The degradation products were kept at specific time interval. To study the kinetics, UV/VIS spectrometer was used for monitoring absorbance change as shown in Figure 22.

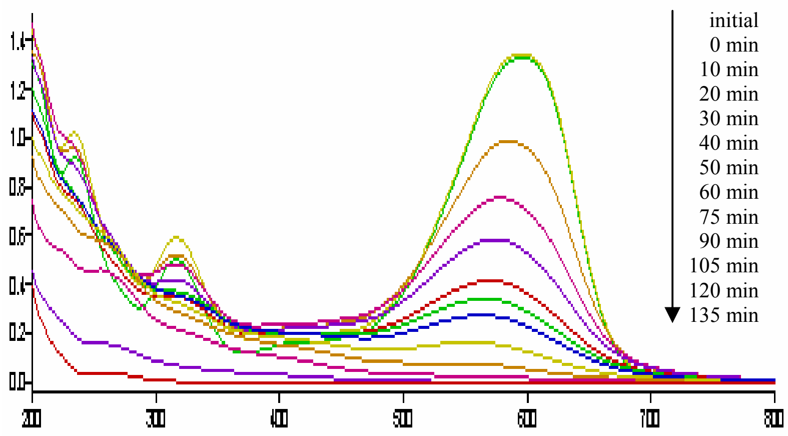

Figure 22 Absorption spectra of 5.20 x 10^{-5} M Trypan Blue at pH 7 (natural) with 1 gL^{-1} of 0.36 wt% gold/TiO_2 suspension following photocatalytic degradation at various irradiation time

The degradation rate of Trypan Blue was monitoring at maximum wavelength, 596 nm, in visible region and it is found to follow first order kinetics. The relative of Trypan Blue remain is presented in exponential line, Figure 23(a). The first order rate constant (k) for degradation of Trypan Blue equals to the slope of $\ln(A/A_0)$ plotted against with irradiation time as shown in straight line, Figure 23(b). As a result, the k value and half-life of first order kinetics were calculated to be 0.0299 and 23.1773 (min^{-1}), respectively.

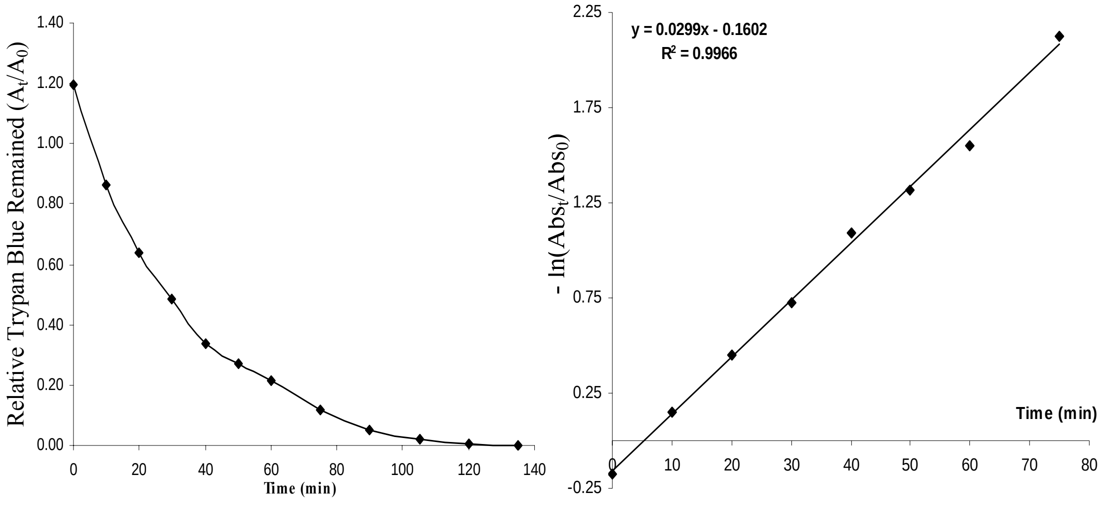

a) b)

Figure 23 a) The exponential decay, and b) the first order kinetics of 5.20 x 10^{-5} M of Trypan Blue, an initial pH 7 in the presence of 0.36 wt% gold/TiO_2 at 1.0 gL^{-1}

4.2 Intermediates study of Trypan Blue

During the experiment, the solution containing Trypan Blue changes into purple, red-brown, yellow and colorless instead of blue. This result may be destruction of Trypan Blue. As mentioned before, the intermediates of the degradation of Trypan Blue would be studied using three techniques:

4.2.1 LC/DAD analysis

The degraded solutions were analyzed according to gradient program as listed in Table 3 after a two-fold dilution. The standard compounds which are expected to be possible intermediates of the degradation of Trypan Blue are studied and their retention time are presented in Table 17. Chromatogram of Trypan Blue at pH 7 is shown in Figure 24. The peak is observed at retention time approximate 9.450 min. After 50 min of irradiation, the peak at this retention time disappears as shown in Figure 25. This result suggests that Trypan Blue was completely destroyed. However, new peaks at approximate 1.580, 2.000 and 2.200 min gradually increase, then these new peaks decrease. These peaks completely disappear after 2 h and 15 min irradiation (Figure 26). By comparison these peaks with known standards, intermediates may be 8-Amino-1-naphthol-3,6-disulfonic acid disodium salt or one of acid compounds. The profile of photodegradation products are presented in Figure 27.

Table 17 The standards and their retention times on LiChrospher®60 RP-select B column

Name	Molecular Structure	Retention time (min)
Oxalic acid	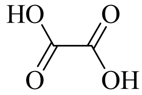	1.752
Maleic acid	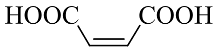	1.784
Succinic acid	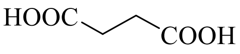	1.866
Tartaric acid	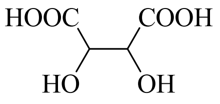	1.837

Table 17 (Cont'd)

Name	Molecular Structure	Retention time (min)
Phthalic acid	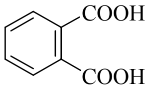	1.967
8-Amino-1-naphthol-3,6-disulfonic acid disodium salt	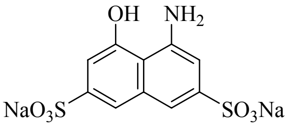	1.936
Anthranilic acid	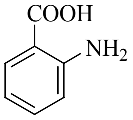	3.821
Benzoic acid	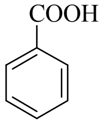	4.397
3-Aminophenol	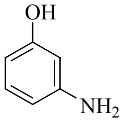	10.347
Phenol	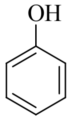	12.952
Benzidine	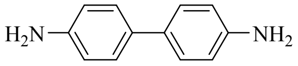	13.547
o-Toluidine	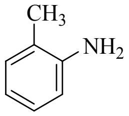	13.731
o-Tolidine	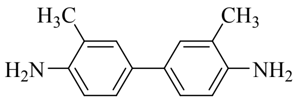	14.219
1-Naphthol	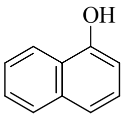	14.472

Table 17 (Cont'd)

Name	Molecular Structure	Retention time (min)
1-Aminonaphthalene	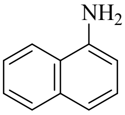	14.517
Naphthalene-1,3,6-trisulfonic acid trisodium salt	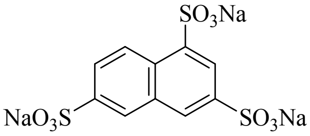	1.584

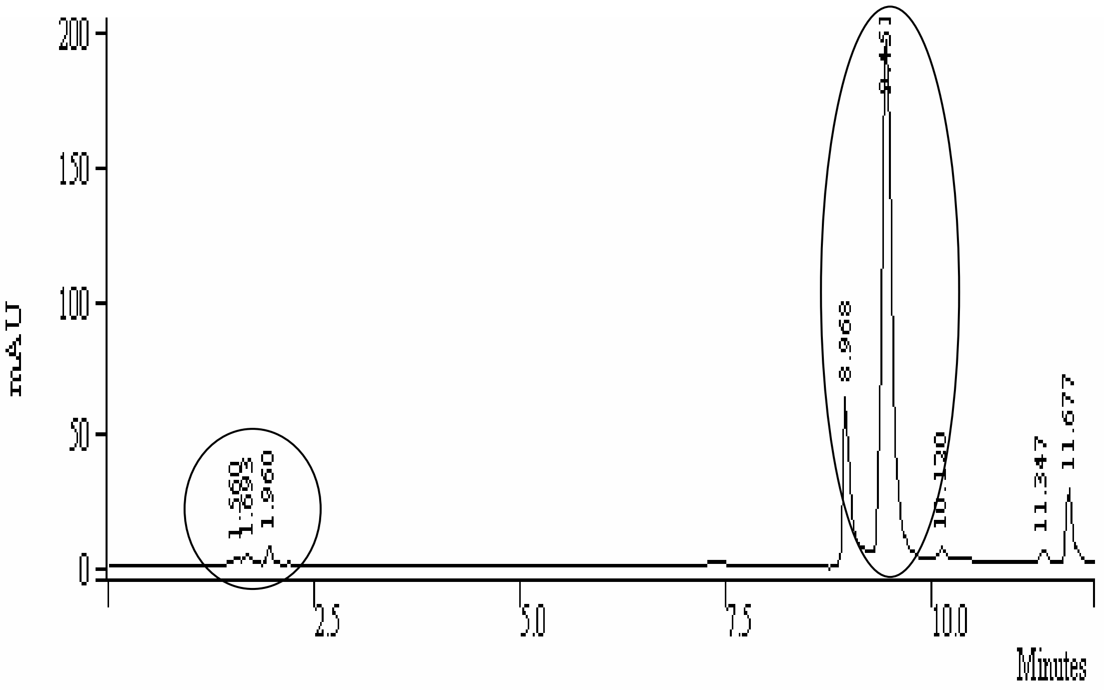

Figure 24 Chromatogram of 5.20 x 10^{-5} M Trypan Blue with 1 gL^{-1} 0.36 wt% gold/TiO_2 suspension at pH 7

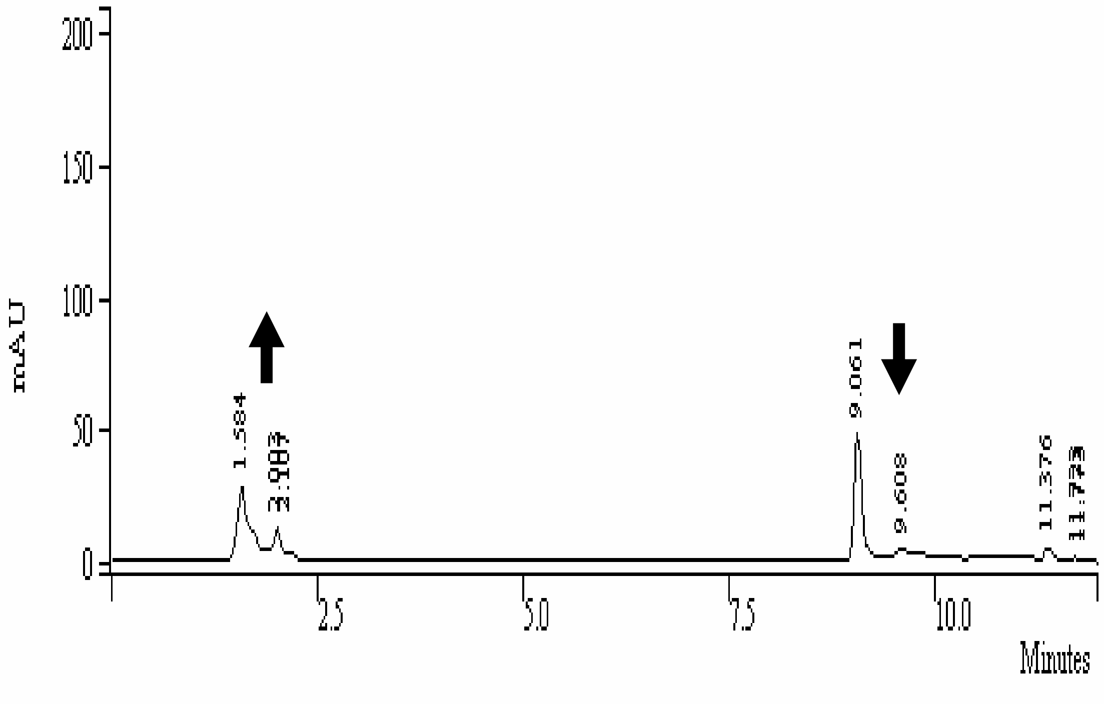

Figure 25 Chromatogram of 5.20 x 10^{-5} M Trypan Blue with 1 gL^{-1} 0.36 wt% gold/TiO_2 suspension at pH 7 after irradiation time of 50 min.

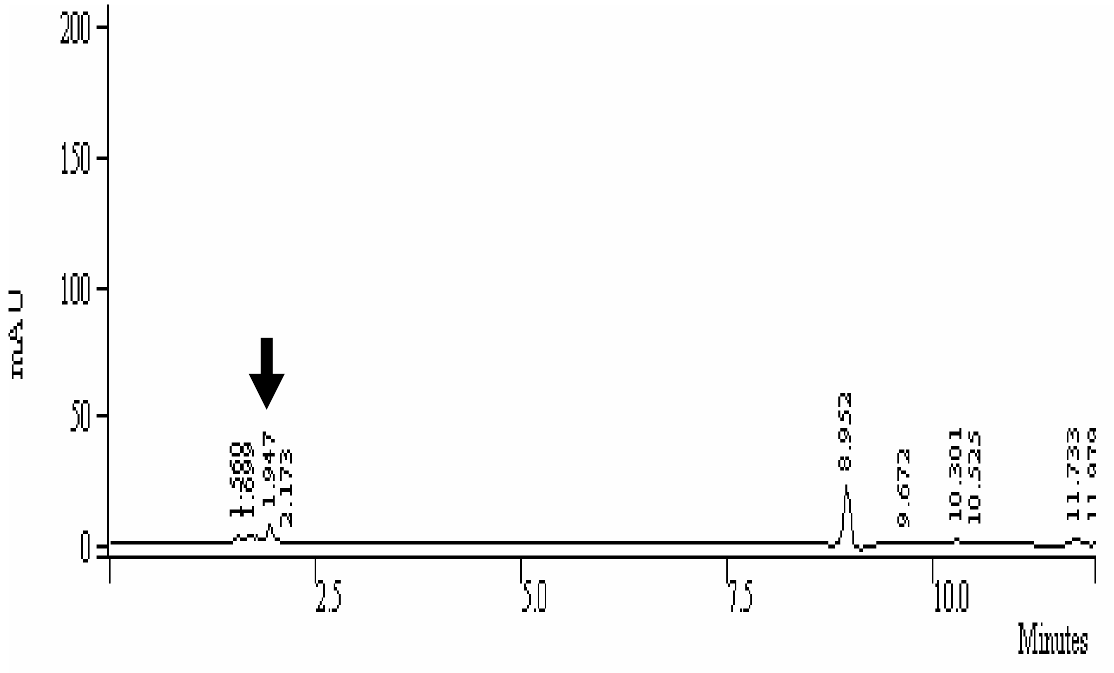

Figure 26 Chromatogram of 5.20 x 10^{-5} M Trypan Blue with 1 gL^{-1} 0.36 wt% gold/TiO_2 suspension at pH 7 after irradiation time of 2 h 15 min.

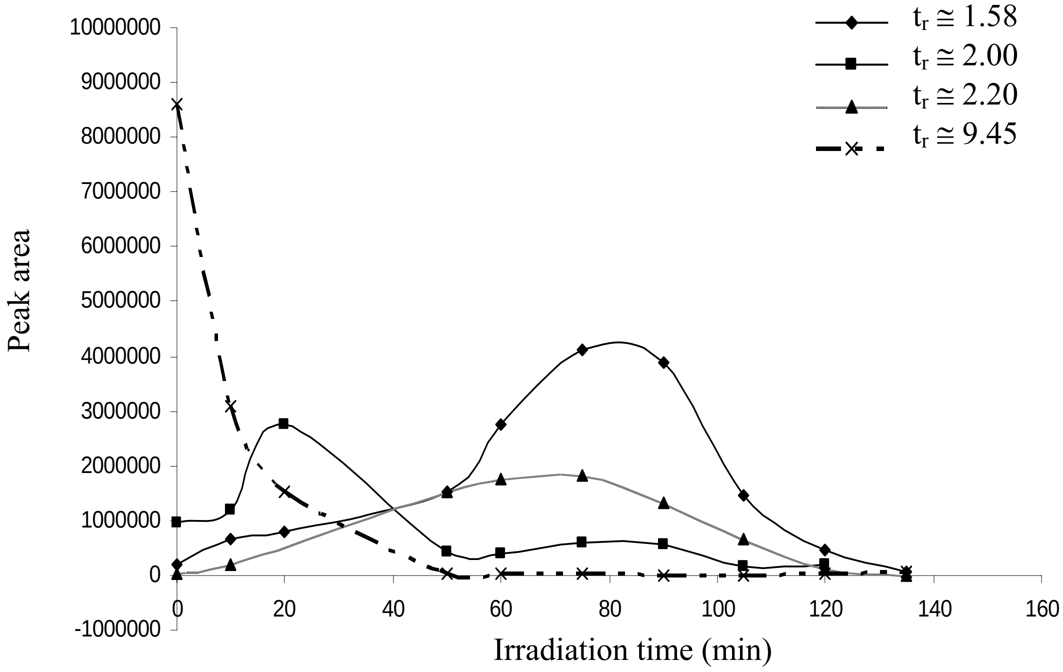

Figure 27 Profile of photodegradation products of Trypan Blue

4.2.2 LC/MS/MS analysis

Table 18 MS/MS transitions and retention time of five aromatic amines and four organic acids studied in this work

Chemical Name	Structure	t_R (min)	MS/MS Transition
NI Mode			
Maleic acid	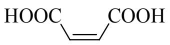	1.74	115([M-H]$^-$)→71([M-H-COO]$^-$)
Anthranilic acid	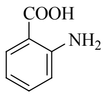	2.58	136([M-H]$^-$)→92([M-H-COO]$^-$)
Benzoic acid	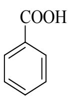	2.67	121([M-H]$^-$)→77([M-H-COO]$^-$)

Table 18 (Cont'd)

Chemical Name	Structure	t_R (min)	MS/MS Transition
PI Mode			
Phthalic acid	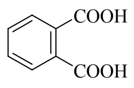	1.69	$167([M+H]^+) \rightarrow 149([M+H-H_2O]^+)$ $167([M+H]^+) \rightarrow 121([M+H- -COOH]^+)$
3-Aminophenol	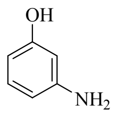	4.25	$110([M+H]^+) \rightarrow 93([M+H-OH]^+)$ $110([M+H]^+) \rightarrow 65([M+H-NH_3- -CO]^+)$
o-Toluidine	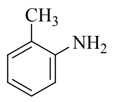	7.33	$108([M+H]^+) \rightarrow 91([M+H-NH_3]^+)$ $108([M+H]^+) \rightarrow 65([M+H-NH_3- -C_2H_2]^+)$
Benzidine	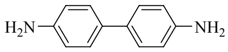	7.75	$185([M+H]^+) \rightarrow 168([M+H-NH_3]^+)$ $185([M+H]^+) \rightarrow 151([M+H-2NH_3]^+)$
o-Tolidine	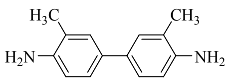	9.90	$213([M+H]^+) \rightarrow 196([M+H-NH_3]^+)$ $213([M+H]^+) \rightarrow 181([M+H-CH_3- -NH_3]^+)$
8-Amino-1-naphthol-3,6-disulfonic acid disodium salt	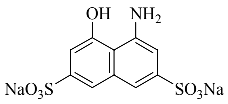	11.57	$319([M+H]^+) \rightarrow 151([M+H-$ $319([M+H]^+) \rightarrow 133([M+H-$

MS/MS transitions and retention time of studied five aromatic amines and four organic acids are summarized in Table 18. The degradation of 2.60 x 10^{-4} M Trypan Blue 50 mL, initial pH 7 in the presence of 1 g/L of 0.36 wt% Au/TiO_2 during the irradiation was monitored. The colorless of solution achieved after 6 h. After 2, 4, 6 and 8 h of irradiation time, the peaks at retention time approximate 1.74 min are observed. Figure 28 shows the chromatograms of Trypan Blue degraded for 6 h and peak at 1.74 min monitored in product ion scan MS/MS. The ions at mass m/z 115 and 71 amu are found. By comparing this peak with the studied standard in Table 18, it may be maleic acid. Figure 29 shows a typical Q1 scan in negative ion mode and product ion scan of the m/z 115 of maleic acid, which the ions at mass m/z 115 and 71 correspond to $[M-H]^+$ and $[M- COOH]^+$, respectively.

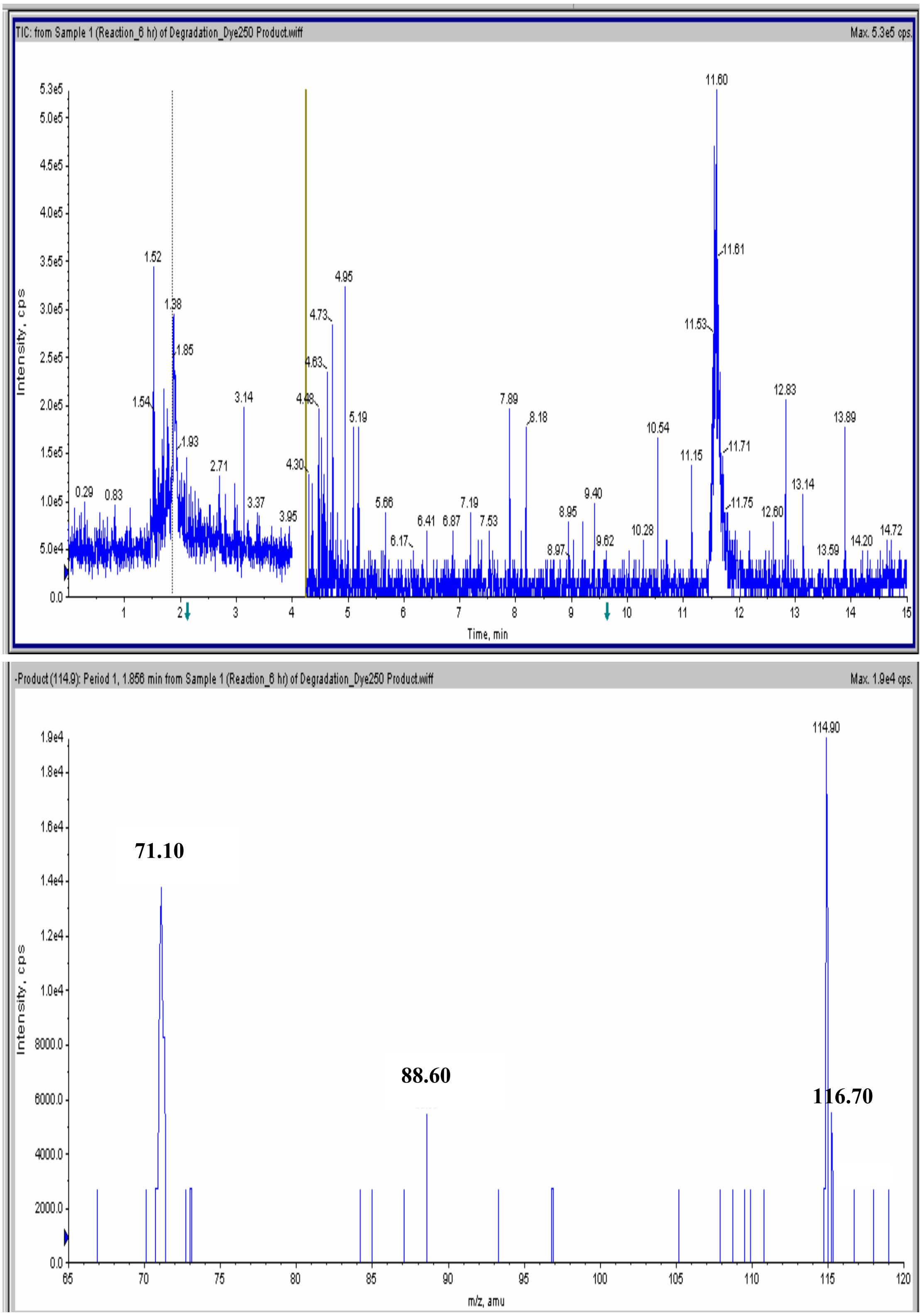

Figure 28 Chromatograms of Trypan Blue degraded for 6 h and peak at 1.856 min monitored in product ion scan MS/MS

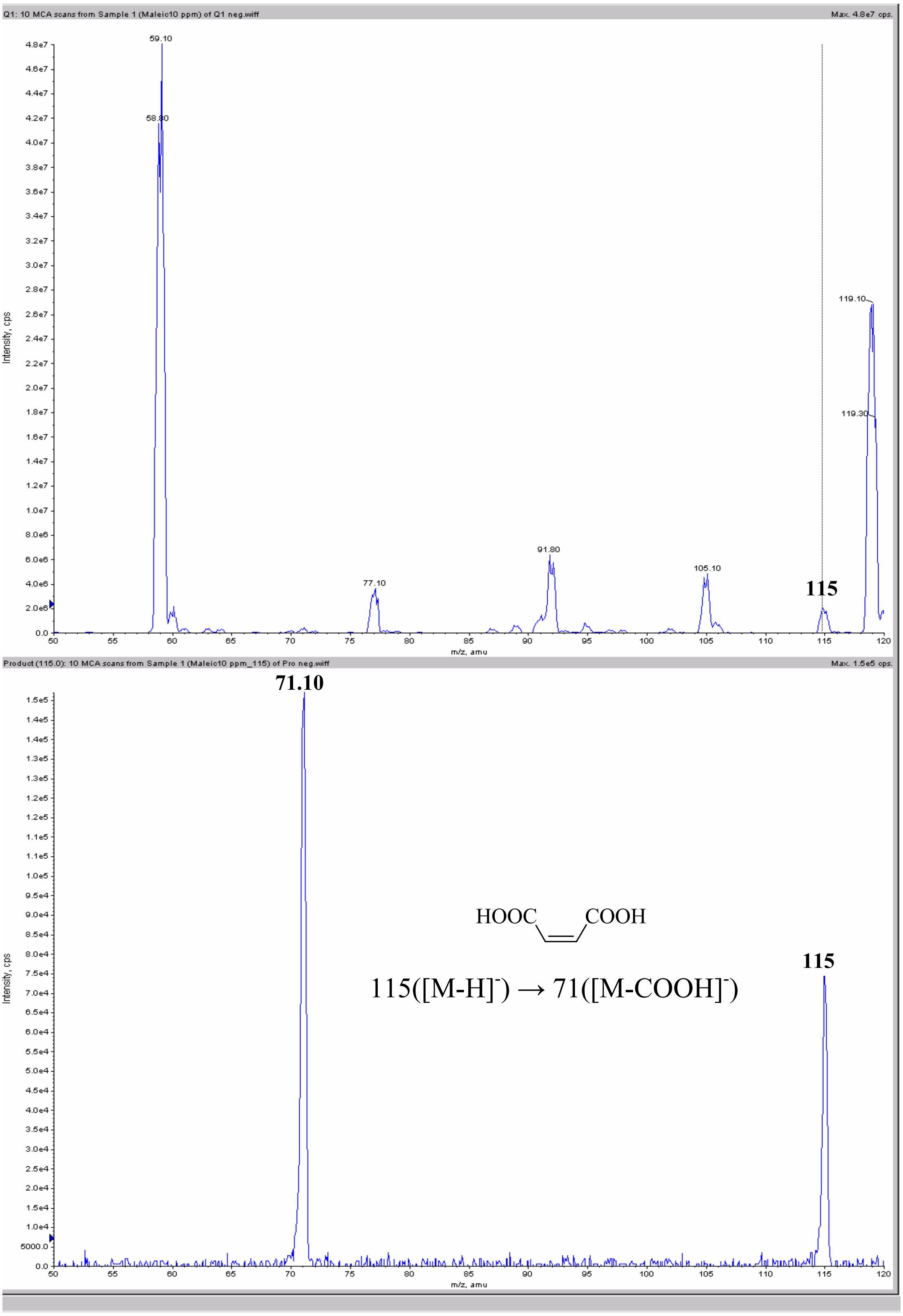

Figure 29 A typical Q1 scan in negative ion mode and product ion scan of the m/z 115 of maleic acid

4.2.3 Ion chromatography analysis

To study the mineralization products of Trypan Blue, the samples collected at the reported irradiation time were analyzed for determination of inorganic molecules including nitrate (NO_3^-), nitrite (NO_2^-), sulfate (SO_4^{2-}) and acid compounds including acetic, formic, succinic, tartaric, maleic, oxalic and phthalic acid. Their retention times and calibration curve data are listed in Table 19. The formation and degradation of reaction products from the Trypan Blue photooxidation are shown in Figure 30, the number below each peak correspond to peak number in Table 19.

Table 19 The retention time and calibration curve data of studied acids and inorganic products

No	Analyte ions and acid molecules	Retention time(min)	Conc. Range (ppm)	Equation Y =	R^2
1	Acetic acid	1.947	0.10 – 0.50	0.5370x + 0.0001	0.9984
2	Formic acid	2.083	0.05 – 0.50	0.6867x + 0.0043	0.9995
3	Succinic acid	2.627		not detected	
4	Nitrite	3.603	0.05 – 0.20	0.3888x - 0.0012	0.9947
5	Nitrate	6.390	0.10 – 5.00	0.4087x + 0.0358	0.9987
6	Tartaric acid	9.227		not detected	
7	Maleic acid	10.483		not detected	
8	Sulfate	11.877	1.00 – 20.00	0.5014x + 0.0618	0.9993
9	Oxalic acid	11.410		not detected	
10	Phthalic acid	12.483		not detected	

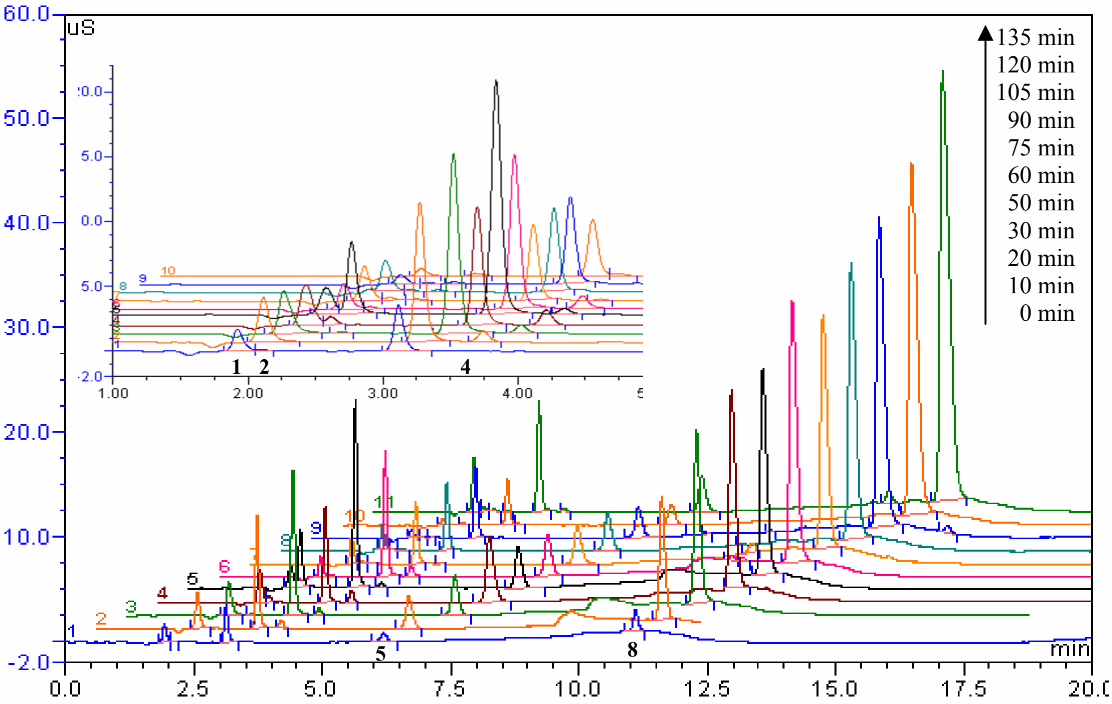

Figure 30 Ion Chromatogram of reaction products of 5.20×10^{-5} M Trypan Blue with 1 gL^{-1} 0.36 wt% gold/TiO_2 suspension at pH 7

The concentrations of these inorganic and acid products are presented in Figure 31. By comparison of retention time of unknown products with that of standards, it is concluded Trypan Blue is mineralized to NO_2^-,NO_3^-, SO_4^{2-} and photodegradated to acetic and formic acid. Sulfate ion is predominant peak which rapidly increase after illumination.

The concentration of sulfate ions continuously increases up to ca. 1.805×10^{-4} M after 135 min of irradiation. The quantity of sulfur (S) is ca. 87 % which lower than that expected from stoichiometry. A substantial amount of sulfur is possible that SO_4^{2-} adsorbed on the photocatalyst surface. Otherwise, the complete mineralization has not occurred at this time. As also observed in Figure 30, only few amounts of nitrate and nitrite ions are produced. The total amount of nitrogen-containing ions presented in solution during the experiment is about 12% of nitrogen that expected from stoichiometry for complete mineralization. Nitrogen-containing ions were evaluated at 30 min of irradiation time due to containing the highest concentration of nitrogen throughout this experiment. It is indicated that nitrogen species remain adsorbed on the catalyst surface, quantities of N_2 and/or NH_3 have been produced and transferred to gas phase. For the other reasons, the formation of the end products should be NH_4^+ which has not been determined or irradiation time is not enough for complete mineralization to CO_2, H_2O and inorganic compounds (Stylidi *et al.*, 2003).

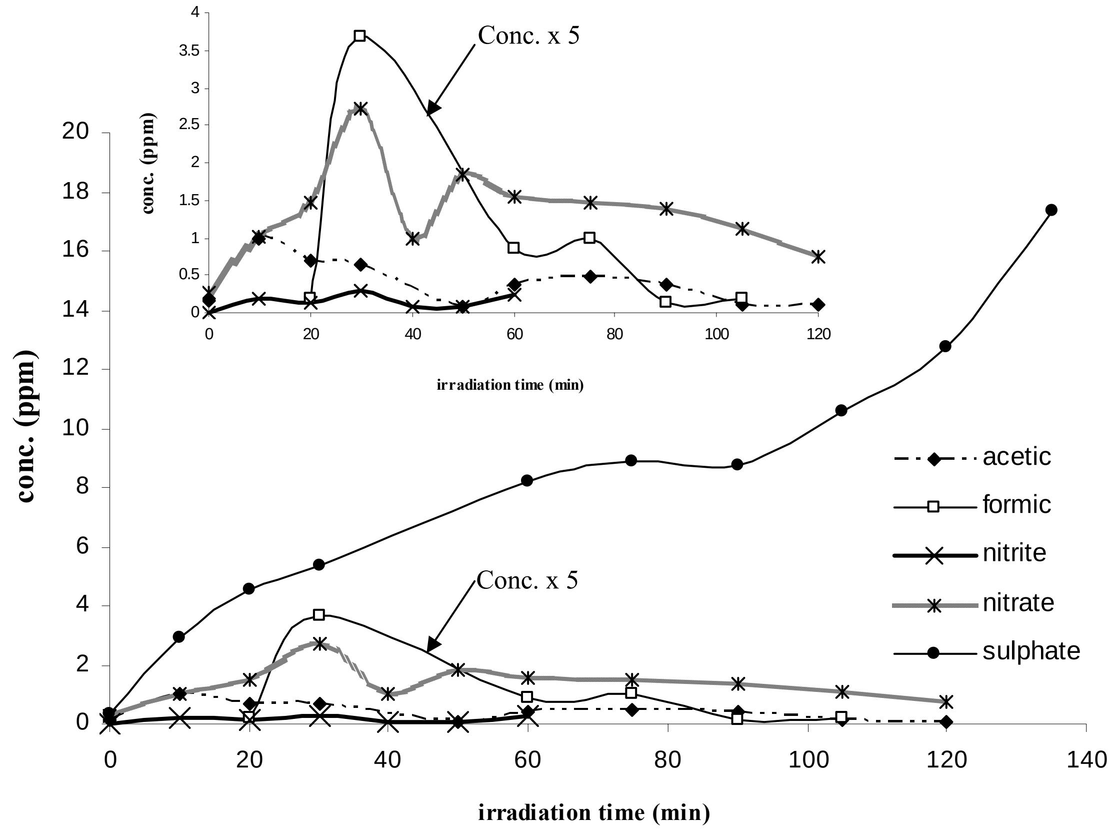

Figure 31 Concentration profile of photodegradation products of Trypan Blue

Consequently, Trypan Blue pollutant can be decomposed through a reaction involving several intermediates, particularly organic acids such as maleic acid together with formation of the inorganic final products (SO_4^{2-}, NO_3^-, NO_2^-, NH_4^+), carbon dioxide and water.

5. Photocatalytic degradation of wastewater

The modified gold/TiO_2 was applied to natural sunlight in the sunny day. Figure 32 shows absorption spectra of Trypan Blue at pH 7 (natural) in the presence of 0.36 wt% gold/TiO_2 and TiO_2 under natural sun light. As a result, photocatalytic degradation of Trypan Blue using improved catalysts ($k = 0.0250\ min^{-1}$) is more efficient than TiO_2 without gold loading ($k = 0.0166\ min^{-1}$).

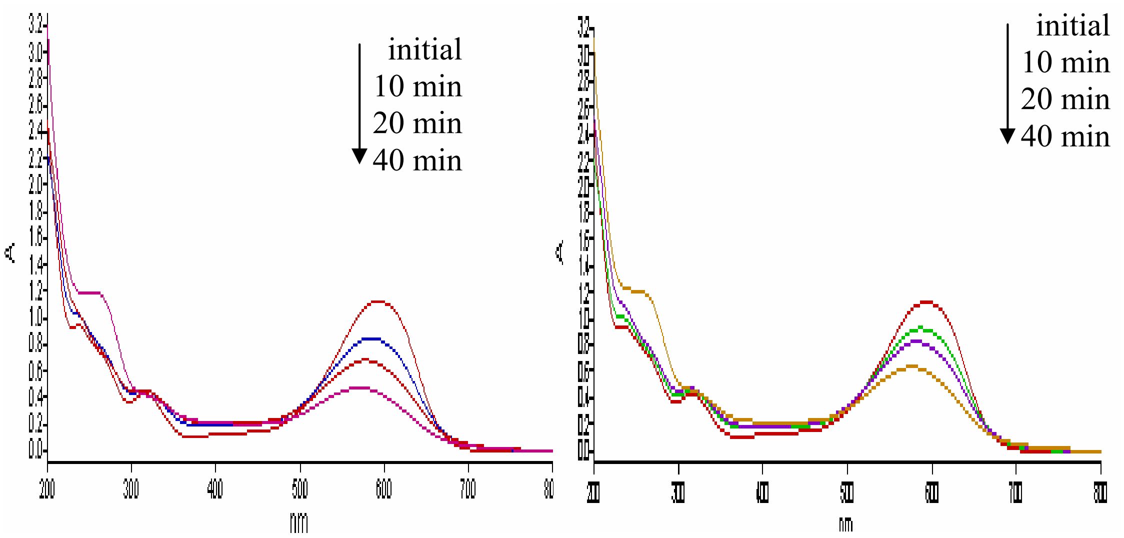

a) b)

Figure 32 Absorption spectra 2.60 x 10^{-5} M Trypan Blue at pH 7 (natural) in the presence of a) 0.36 wt% gold/TiO_2 and b) TiO_2, under natural sun light

The method obtained was applied successfully as shown in Figure 33 to reductive dye wastewater with k = 0.0098 min^{-1} (R^2 = 0.9912) as shown in Figure 34. In addition, the formation of NO_3^- and SO_4^{2-} are described in Figure 35. Obviously, the photodegradation and mineralization rate of wastewater is very slow comparing with aqueous Trypan Blue.

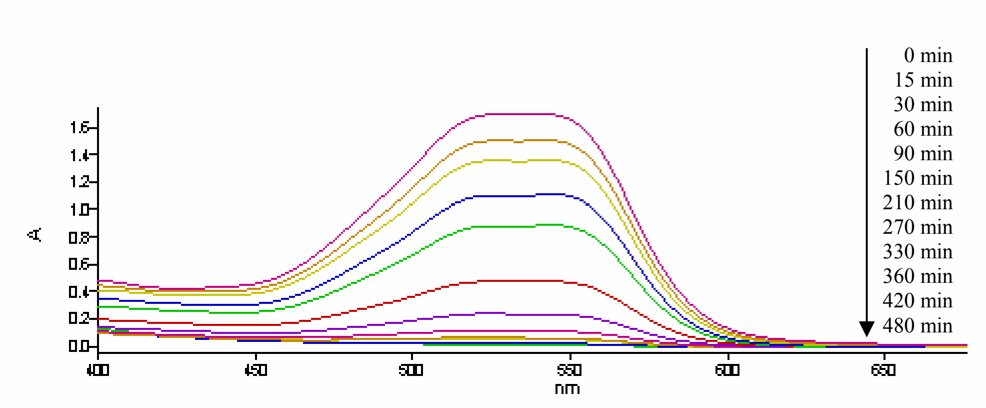

Figure 33 Absorption spectra of textile wastewater, reactive dye group, with 1 gL^{-1} of 0.36 wt% gold/TiO_2 suspension following photocatalytic degradation at various irradiation time

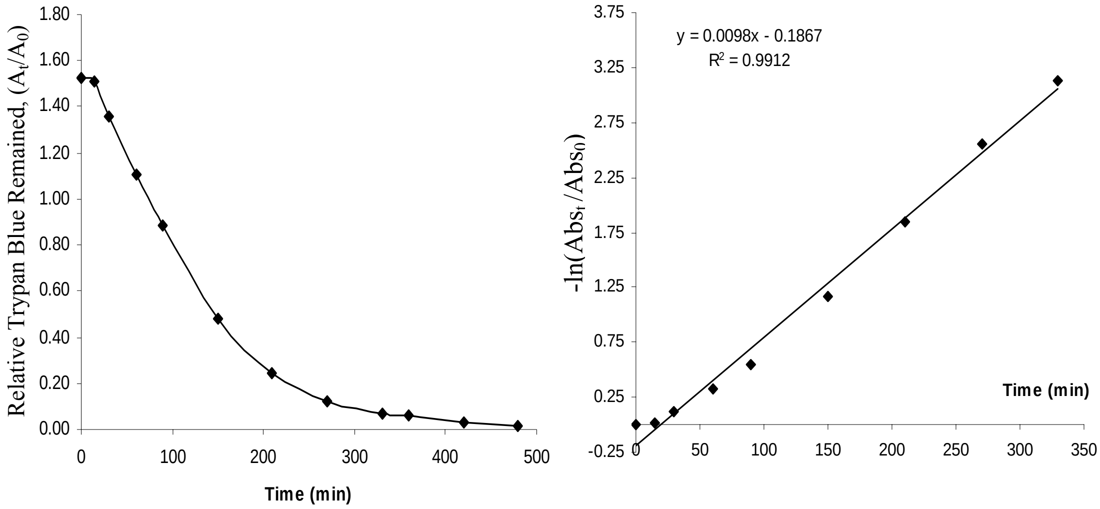

a)

b)

Figure 34 a) The exponential decay, and b) the first order kinetics of reactive dye wastewater, pH value was adjusted to 7, in the presence of 0.36 wt% gold/TiO_2 at 1.0 gL^{-1}

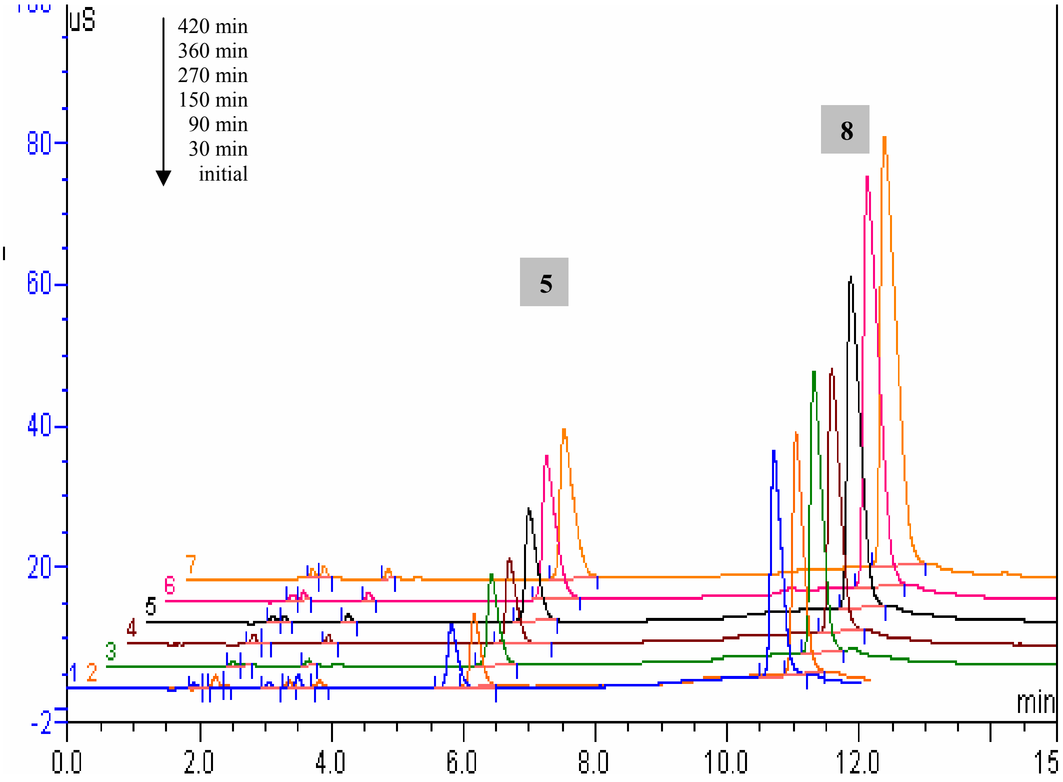

Figure 35 Chromatogram of textile wastewater, reactive dye group, with 1 gL^{-1} of 0.36 wt% gold/TiO_2 suspension following photocatalytic degradation at various irradiation time

Trypan Blue spiked in reactive dye wastewater was studied to confirm the difficulty of dye degradation in wastewater. The decrease of Trypan Blue was monitored at retention time of 8.605 min. The disappearance of this peak would occur after irradiation for more than 2 h as shown in Figure 36 and 37. By contrast, 5.20 x 10^{-5} of Trypan Blue in aqueous solution was degraded faster than Trypan Blue in wastewater at the same concentration. It was known that effluent from the dyeing and finishing process in textile industry contain strong color, high amounts of surfactants, dissolved solids, high pH and possibly heavy metals (Arslan and Balcioglu, 1999), so, these causes affect to the decrease in efficiency of photodegradation.

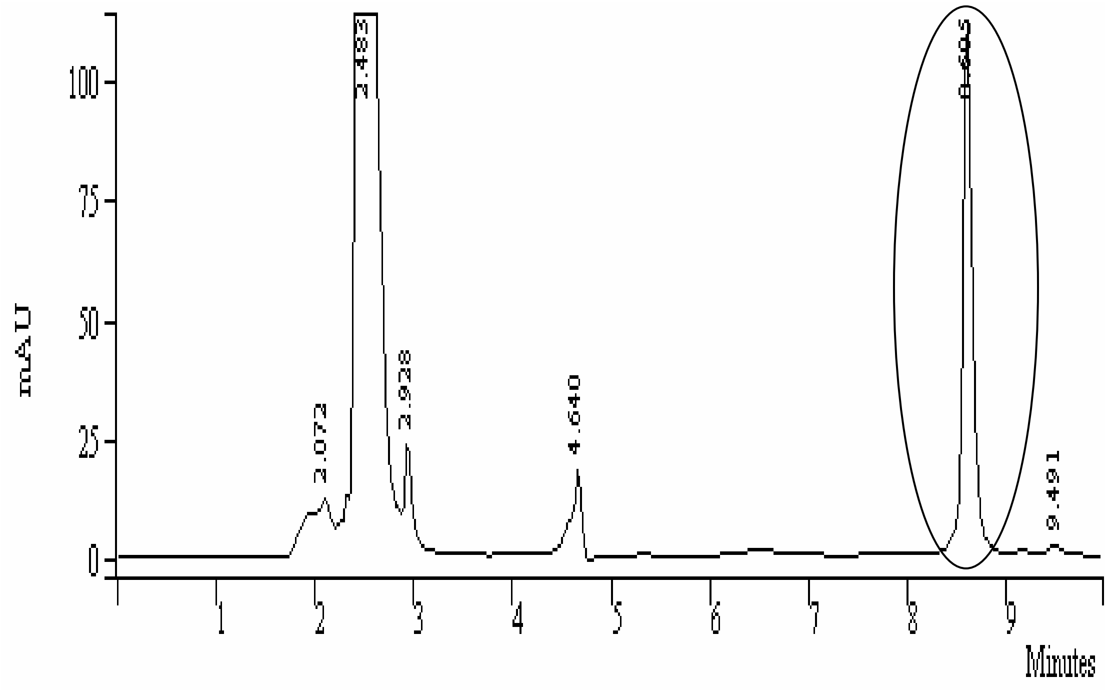

Figure 36 Chromatogram of 5.20 x 10^{-5} M Trypan Blue spiked in reactive dye wastewater in the presence of 1 gL^{-1} 0.36 wt% gold/TiO_2

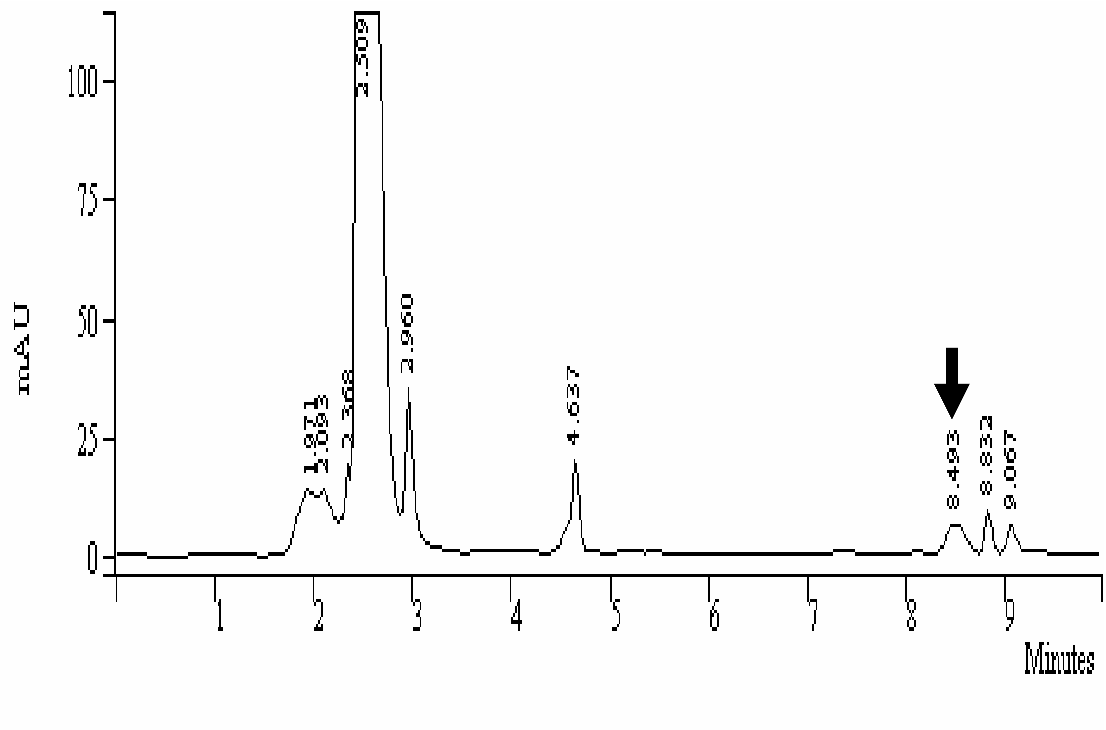

Figure 37 Chromatogram of 5.20 x 10^{-5} M Trypan Blue spiked in reactive dye wastewater in the presence of 1 gL^{-1} 0.36 wt% gold/TiO_2.after 2 h of irradiation time

CONCLUSIONS

- Au/TiO_2 was prepared and its activity for phocatalytic degradation of Trypan Blue is seven fold higher than that of undoped TiO_2.

- The rate of disappearance of the dye follows first order kinetics under simulating solar light.

- Maleic acid, formic acid, acetic acid, NO_2^-, NO_3^- and SO_4^{2-} are photodegradation products.

- The method is applied successfully to photodegrade wastewater containing reactive dyes.

SUGGESTION FOR FUTURE WORK

- Pathway of photodegradation of Trypan Blue will be further studied by monitoring all intermediates formed during the photodegradation of Trypan Blue.

LITERATURE CITED

Arabatzis, I.M., T. Stergiopoulos, D. Andreeva, S. Kitova, S.G. Neophytides and P. Falaras. 2003. Characterization and photocatalytic activity of Au/TiO_2 thin films or azo-dye degradation. **Journal of Catalysis**. 220:127-135.

Arslan, I and I. A. Balcioglu. 1999. Degradation of commercial reactive dyestuffs by heterogenous and homogenous advanced oxidation processes: a comparative study. **Dyes and Pigments.** 43:95-108.

Augugliaro, V., Claudio Baiocchi, Alessandra Bianco Prevot, Elisa García-López, Vittorio Loddo, Sixto Malato, Giuseppe Marci, Leonardo Palmisano, Marco Pazzi, Edmondo Pramauro. 2002. Azo-dyes photocatalytic degradation in aqueous suspension of TiO_2 under solar irradiation Azo-dyes photocatalytic degradation in aqueous suspension of TiO_2 under solar irradiation. **Chemosphere.** 49:1223–1230.

Baiocchi, C., M. C. Brussino, E. Pramauro, A. B. Prevot, L. Palmisano, G. Marcì. 2002. Characterization of methyl orange and its photocatalytic degradation products by HPLC/UV–VIS diode array and atmospheric pressure ionization quadrupole ion trap mass spectrometry. **International Journal of Mass Spectrometry**. 214:247–256.

Bamwenda, G. R., S. Tsubota, T. Nakamura and M. Haruta. 1995. Photoassisted hydrogen production from a water-ethanol solution: a comparison of activities of Au-TiO_2 and Pt-TiO_2. **J. Photochem. Photobiol. A: Chem**. 89:177-189.

Bandara, J., J. A. Mielczarski and J. Kiwi. 1999. 2. Photosentized Degradation of Azo Dyes on Fe, Ti, and Al Oxides. Mechanism of Charge Transfer during the Degradation. **Langmuir**. 15:7680-7687.

Bauer, C., P. Jacques and A. Kalt, 2001. Photooxidation of an azo dye induced by visible light Incident on the surface of TiO_2. **J. Photochem Photobiol A: Chem**. 140:87-92.

Chun, H. and W. Yizhong. 1999. Decolorization and biodegradability of photocatalytic treated azo dyes and wool textile wastewater. **Chemosphere**. 39(12):2107-2115.

Daneshvar, N., D. Salari, A.R. Khataee. 2003. Photocatalytic degradation of azo dye acid red 14 in water:investigation of the effect of operational parameters. **J. Photochem. Photobiol. A: Chem.** 157:111–116.

Davis, R.J., J.L. Gainer, G. O'Neal and W. Wu. 1994. Photocatalytic decolorization of water dyes. **Water Environment Research**. 66(1):50-53.

Dawson, A., and P. V. Kamat. 2001. Semiconductor-Metal Nanocomposites. Photoinduced Fusion and Photocatalysis of Gold-Capped TiO_2 (TiO_2/Gold) Nanoparticles. **J. Phys. Chem. B**. 105:960-966.

Galindo, C., P. Jacques and A. Kalt. 2000. Photodegradation of the aminoazobenzene acid orange 52 by three advanced oxidation processes: UV/H_2O_2, UV/TiO_2 and VIS/TiO_2 comparative mechanistic and kinetic investigations. **J. Photochem. Photobiol. A: Chem.** 130:35-47.

Guillard, C., H. Lachheb, A. Houas, M. Ksibi, E. Elaloui, J.-M. Herrmann. 2003. Influence of chemical structure of dyes, of pH and of inorganic salts on their photocatalytic degradation by TiO2 comparison of the efficiency of powder and supported TiO_2. **J. Photochem. Photobiol. A: Chem.** 158:27–36.

Halmann, M. M., 1996. **Photodegradation of Water Pollutants.** CRC Press, Boca Raton, Florida. 301p.

Hu, C., Y. Tang, Z. Jiang , Z. Hao, H. Tang, P. K. Wong. 2003. Characterization and photocatalytic activity of noble-metal-supported surface TiO_2/SiO_2. **Applied Catalysis A: General.** 253:389–396.

Ince, N. H. 1997. UV/H_2O_2 Degradation and Toxicity Reduction of Textile Azo Dyes: Remazol Black-B, a case Study. **J. Adv. Oxid. Technol.** 2(3):442-448.

Kiriakidou, F., D.I. Kondarides and X.E. Verykios. 1999. The effect of operational parameterss and TiO_2-doping on the photocatalytic degradation of azo-dyes. **Cataysis Today**. 54:119-130.

Konstantinou, I.K. and T.A. Albanis. 2004. TiO_2-assisted photocatalytic degradation of azo dyes in aqueous solution: kinetic and mechanistic investigations: A review. **Applied Catalysis B: Environmental**. 49:1-14.

Lachheb, H., E. Puzenat, A. Houas, M. Ksibi, E. Elaloui, C. Guillard, J.-M. Herrmann. 2002. Photocatalytic degradation of various types of dyes (Alizarin S, Crocein Orange G, Methyl Red, Congo Red, Methylene Blue) in water by UV-irradiated titania. **Applied Catalysis B: Environmental.** 39:75–90.

Li, F.B. and X.Z. Li. 2002. Photocatalytic properties of gold /gold ion-modified titanium dioxide for wastewater treatment. **Applied Catalysis A: General.** 228:15-27.

Mallick, K., M. J. Witcomb and M.S. Scurrell. 2004. Supported gold catalysts prepared by in situ reduction technique: preparation, characterization and catalytic activity measurements. **Applied Catalysis A: General**. 259:163-168.

Nasr, C., K. Vinodgopal, L. Fisher, S. Hotchandani, A.K. Chattopadhyay and P.V. Kamat. 1996. Environmental Photochemistry on Semiconductor Surfaces. Visible Light Induced Degradation of a Textile Diazo Dye, Naphthol Blue Black, on TiO_2 Nanoparticles. **J. Phys. Chem.** 100: 8436-8442.

Neppolian, B., H.C. Choi, S. Sakthivel, B. Arabindoo and V. Murugesan. 2002. Solar light induced and TiO_2 assisted degradation of textile dye reactive blue 4. **Chemosphere.** 46:1173–1181.

Nogueira, R.F.P. and W.F. Jardim. 1993. Photodegradation of methylene blue using solar light and semiconductor (TiO_2). **Journal of Chemical Education.** 70:861-862.

Poulios, I. and I. Tsachpinis. 1999. Photodegradation of the textile dye Reactive Black 5 in the presence of semiconducting oxides. **J. Chem Technol Biotechnol.** 74:349-357.

Qamar, M., M. Saquib and M. Muneer. 2005. Photocatalytic degradation of two selected dye chromotrope 2B and amido black 10B, in suspensions of titanium dioxide. **Dyes and Pigments.** 65:1-9.

Reutergårdh, L.B. and M. Iangphasuk. 1997. Photocatalytic decolourization of reactive azo dye: a comparison between TiO_2 and CdS photocatalysis. **Chemosphere.** 35:585-596.

Sakthivel, S., B. Neppolian, M.V. Shankar, B. Arabindoo, M. Palanichasmy and V. Murugesan. 2003. Solar photocatalytic degradation of azo dye: comparison of photocatalytic efficiency of ZnO and TiO_2. **Solar Energy Materials & Solar Cells.** 77:65-82.

__________, M.V. Shankar, M. Palanichamy, B. Arabindoo and V. Murugesan. 2002. Photocatalytic decomposition of leather dye Comparative study of TiO_2 supported on alumina and glass beads. **J. Photochem. Photobiol. A: Chem.** 148:153–159.

Sakthivel, S., M.V. Shankar, M. Palanichamy, B. Arabindoo, D.W. Bahnemann, V. Murugesan. 2004. Enhancement of photocatalytic activity by metal depoitions: characterisatsion and photonic efficiency of Pt, Au and Pd depoited on TiO_2 catalyts. **Water Research**. 38:3001-3008.

Sangchakr, B., T. Hisanaga, K. Tanaka. 1995. Photocatalytic degradation of sulfonated aromatics in TiO_2 suspension. **J. Photochem Photobiol. A: Chem.** 85:187-190.

Saquib, M. and M. Muneer. 2003. TiO_2-mediated photocatalytic degradation of a triphenylmethane dye (gentian violet), in aqueous suspensions. **Dyes and Pigments**. 56:37-49.

Shu, H.-Y., and C.-R. Huang. 1995. Degradation of commercial azo dyes in water using ozonation and UV enhanced ozonation process. **Chemosphere.** 31(8):3813-3825.

Silva, C. G. da, J. L. Faria. 2003. Photochemical and photocatalytic degradation of an azo dye in aqueous solution by UV irradiation. **J. Photochem. Photobiol. A: Chem.** 155:133–143.

Slokar, Y.M. and A. Majcen Le Marechal. 1998. Methods of Decoloration of Texile Wastewaters. **Dyes and Pigments**. 37(4):335-356.

Stylidi, M., D.I. Kondarides and X.E. Verykios. 2003. Pathways of solar light-induced photocatalytic degradation of azo dyes in aqueous TiO_2 suspensions. **Applied Catalysis B: Environmental**. 40:271–286.

Subramanian, V., E. E. Wolf and P. V. Kamat. 2003. Influence of Metal/Metal Ion Concentration on the Photocatalytic Activity of TiO_2-Au Composite Nanoparticles. **Langmuir.** 19(2):469-474.

Tang, W. Z. and H. An. 1995. UV/TiO_2, Photocatalytic Oxidation of Commercial Dyes in Aqueous Solutions. **Chemosphere.** 31(9):41574170.

_________, Z. Zhang, A. Huren, M. O. Quintana and D. F. Torres. 1997. TiO_2/UV Photodegradation of azo dyes in aqueous solutions. **Environ. Technol.** 18:1-12.

Tanaka. K., K. Padermpole and T. Hisanaga. 2000. Photocatalytic Degradation of Commercial Azo Dyes. **Wat. Res.** 34(1):327-333.

Venkatadri, R., and R. W. Peters. 1993. Chemical Oxidation Technologies: Ultraviolet Light/Hydrogen Peroxide, Fenton's Reagent, and Titanium Dioxide-Assisted Photocatalysis. **Haz. Waste & Haz. Mater**. 10(2):107-149.

Vinodgopal, K., I. Bedja, S. Hotchandani and P.V. Kamat. 1994. A Photocatalytic Approach for the Reductive Decolorization of Textile Azo Dyes in colloidal semiconductor suspensions. **Langmuir.** 10:1767-1771.

__________ and Wynkoop, D. E. 1996. Environmental Photochemistry on Semiconductor Surfaces: Photosensitized Degradation of a Textile Azo Dye, Acid Orange 7, on TiO_2 Particles Using Visible Light. **Environ. Sci. Technol**. 30(5):1660-1666.

Wang, C.-y., C.-y. Lui, X. Zheng, J. Chen and T. Shen. 1997. The surface chemistry of hybrid nanometer-sized particles II. Characterization and Microstructure of Au Clusters supported on TiO_2. **J. of colloid and interface science.** 191:464-47.

____1998. The surface chemistry of hybrid nanometer-sized particles I. Photochemical deposition of gold on ultrafine TiO_2 particles. **Colloids Surfaces A: Physicochem. Eng. Aspects.** 131:271-280.

Xu, Y. and C.H. Langford. 2001. UV- or Visible-Light-Induced Degradation of X3B on TiO2 Nanoparticles: The Influence of Adsorption. **Langmuir.** 17:897-902.

Zamora, P. P., A. Kunz, S. G. de Moraes, R. Pelegrini, P. de C. Molelro , J. Reyes and N. Duran. 1999, Degradation of reactive dyes I. a comparative study of ozonation, enzymatic and photochamical process. **Chemosphere**. 38(4):835-852.

Zanella, R., S. Giorgio, C.-H. Shin, C. R. Henry and C. Louis. 2004. Characterization and reactivity in CO oxidation of gold nanoparticles supported on TiO_2 prepared by deposition-precipitation with NaOH and urea. **Journal of Catalysis**. 222:357-367.